Linköping University | Department of Electrical Engineering,
Master's thesis, 30 ECTS | Electrical Engineering
2020 | LITH-ISY-EX–-20/5323--SE

Modeling and lateral control of tractor-trailer vehicles during aggressive maneuvers

Modellering och lateral reglering av lastbilsfordon under aggressiva manövrar

Carl Hynén Ulfsjöö
Theodor Westny

Supervisor : Oskar Ljungqvist, ISY, Linköpings universitet
Examiner : Daniel Axehill, ISY, Linköpings universitet

External supervisor : Niclas Evestedt, Embark Trucks Inc

LINKÖPING UNIVERSITY

Linköpings universitet
SE–581 83 Linköping
+46 13 28 10 00 , www.liu.se

Upphovsrätt

Copyright

Abstract

In the last decades, the development of self-driving vehicles has rapidly increased. Improvements in algorithms, as well as sensor and computing hardware have led to self-driving technologies becoming a reality. It is a technology with the potential to radically change how society interacts with transportation. One crucial part of a self-driving vehicle is control schemes that can safely control the vehicle during evasive maneuvers.

This work investigates the modeling and lateral control of tractor-trailer vehicles during aggressive maneuvers. Models of various complexity are used, ranging from simple kinematic models to complex dynamic models, which model tire slip and suspension dynamics. The models are evaluated in simulations using TruckMaker, which is a high fidelity vehicle simulator.

Several lateral controllers are proposed based on Model predictive control (MPC) and linear-quadratic (LQ) control techniques. The controllers use different complex prediction models and are designed to minimize the path-following error with respect to a geometric reference path. Their performance is evaluated on double lane change maneuvers of various lengths and with different longitudinal speeds. Additionally, the controllers' robustness against changes in trailer mass, weight distribution, and road traction is investigated.

Extensive simulations show that dynamic prediction models are necessary to keep the control errors small when performing maneuvers that result in large lateral accelerations. Furthermore, to safely control the tractor-trailer vehicle during high speeds, it is a necessity to include a model of the trailer dynamics. The simulation study also shows that the proposed LQ controllers have trouble to evenly balance tractor and trailer deviation from the path, while the MPC controllers handle it much better. Additionally, a method for approximately weighting the trailer deviation is shown to improve the performance of both the LQ and MPC controllers. Finally, it is concluded that an MPC controller with a dynamic tractor-trailer model is robust against model errors, and can become even more robust by tuning the controller weights conservatively.

Acknowledgments

First of all, we would like to thank our examiner Daniel Axehill, and our supervisors, Niclas Evestedt and Oskar Ljungqvist for guidance and encouragement throughout this work. Special thanks to Oskar Ljungqvist for constant constructive feedback and for your enthusiasm.

Thanks to the people at Embark Trucks for the incredible opportunity by bringing us to Silicon valley and letting us be a part of the industry forefront. Special thanks to Somudro Gupta with the planning and controls team for ever fruitful discussions and support in this work. Finally, thanks to our friends and families for support in all our endeavors!

Contents

Nomenclature

Acronyms

COM	Center of mass
LQR	Linear quadratic regulator
MPC	Model predictive control
OCP	Optimal control problem

Symbols

α_i	Tire slip angle of tire i
β_i	Sideslip angle of body i
δ_f	Steer angle
Γ	Articulation angle
ϕ_i	Roll angle of body i
ψ_i	Yaw angle of body i
$\psi_{i,e}$	Heading error of body i
a_{ij}	Distance from center of mass of body i to axle j counted from front
b_i	Distance from center of mass of body i to hitch point
$C_{\alpha,i}$	Cornering stiffness of tire i
d	Cross-track error
d_i	Roll damping of i body
d_t	Cross-track error of trailer
$F_{y,i}$	Lateral force of tire i
h_i	Height of center of mass over roll center of body i
$I_{xx,i}$	Roll moment of inertia of sprung mass of body i
$I_{zz,i}$	Yaw moment of inertia of mass of body i
k_ϕ	Roll stiffness of hitch joint
k_i	Roll stiffness of i body
m_i	Mass of mass of body i
$m_{s,i}$	Sprung mass of body i
v	Velocity of tractor
v_x	Longitudinal velocity of tractor
v_y	Lateral velocity of tractor
X	x-position of tractor center of mass
Y	y-position of tractor center of mass

1 Introduction

This thesis is concerned with modeling and automatic lateral control of tractor-trailer vehicles. This chapter is dedicated to give an introduction to the work.

1.1 Background

The development of self-driving vehicles has made an incredible stride in the last decades. Although the idea of self-driving cars has been around since the start of the 20th century, it is not until recently that it seemed like a real possibility. A major milestone along the way was the first DARPA Grand Challenge in 2004 [1]. With the objective to autonomously follow a 240 km off-road course, none of the 15 robot vehicles that had entered, finished the race. As no winner could be declared, a second DARPA challenge was scheduled for 2005 [2]. A major breakthrough in field was made that day as all but one of the 23 finalists finished the race. With the DARPA Urban Challenge in 2007 [3], the competition was set in an urban setting. The vehicles were required to complete a 96 km long course while obeying traffic regulations and negotiating other agents as well as obstacles along the road. The event proved that considerable progress had been made since 2004, as 6 teams finished the challenge, showing that fully autonomous driving is a possibility.

The improvements in technology and hardware availability have further fueled the start of many companies and research groups. The possibilities of self-driving cars are numerous, the development of them however, is not without challenges. In a fast-evolving industry, many companies have failed in the race. However, optimism is not unmotivated as several companies have shown commercial success in both taxi businesses and freight-carrying operations. With the recent success of many companies, the goal of self-driving road vehicles is getting closer to reality. However, as the industry matures, the demands of the public are becoming more vocal.

With the increased interest in the commercialization of autonomous vehicles, developing systems that meet the safety demands has become an important mission for both academia and industry alike. One part of the problem is the implementation of control schemes that can safely control the vehicle's behavior during evasive maneuvers.

For the autonomous trucking industry, the importance of systems that can handle safety-critical scenarios cannot be overstated. Compared to the passenger car industry, the addition of a trailer requires more comprehensive models that may add substantial complexity to the problem. When operating during high-speeds, dynamic

effects of both the tractor and trailer may need to be incorporated in the controller to produce a safe behavior.

1.2 Problem formulation

This thesis aims to investigate how models of varying degrees of complexity can improve lateral control of a tractor-trailer system during aggressive maneuvers. Additionally, different methods for lateral control should also be evaluated in combination with these models. This thesis aims to answer the following questions:

- How well do models of varying complexity predict the lateral behavior of the system?
- How is controller performance affected by different models?
- How well do different controllers perform during aggressive maneuvers?
- How robust are the different controllers against parameter uncertainty?

1.3 Related work

Modeling of car-like vehicles has been an active research field during the past decades. For passenger cars, kinematic models are often used in the literature for automatic steering applications [4, 5, 6]. Corresponding models for tractor-trailer vehicles are extensively covered in [7], where a method is presented for deriving models of the general n-trailer. Kinematic models of articulated vehicles have been used successfully for both planning and control applications [8, 9, 10]. Substantial research has been done in dynamic modeling of tractor-trailer combinations at various complexity [11, 12, 13, 14, 15] and a comparative evaluation between lateral dynamic models for tractor-trailer systems are done in [16].

Automatic control of car-like vehicles is widely covered in the literature. In [4], various control schemes are suggested for self-driving, including pure-pursuit, linear quadratic control, and model predictive control. The former two, are evaluated for automatic steering in [17]. In [18], kinematic and dynamic models are compared for control design using a model predictive control approach. A comparative study of linear quadratic control and model predictive control for path-following applications is done in [19]. Low speed path-following of a tractor-trailer system using a model predictive control approach is done in [20]. For high speed applications the focus of tractor-trailer vehicles have been mostly on stability control [21, 22], although extensive work has been done on lateral control as well [23, 24, 25].

1.4 System overview

An overview of a typical system architecture for an autonomous vehicle is presented in Figure 1.1. Inspired and adapted from [9, 26, 27]. On a high level it consists of three distinct software modules, the planner, the controller and the perception module.

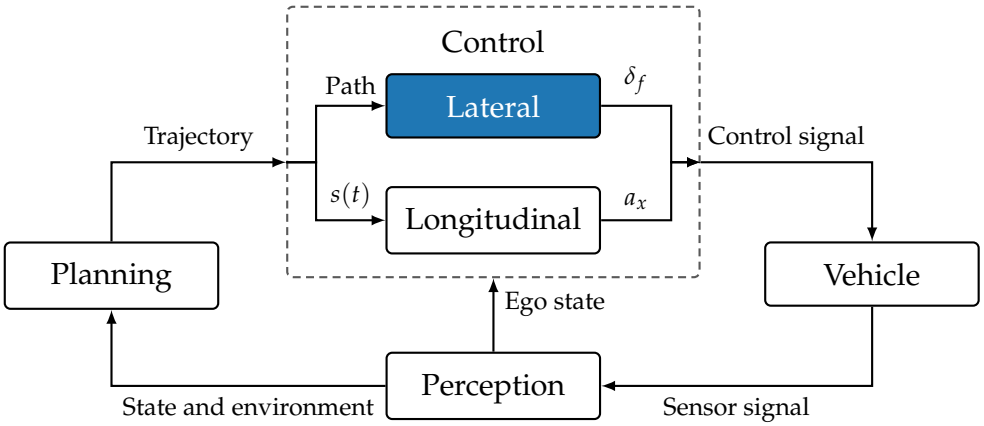

Figure 1.1: The complete system and its underlying components.

The planning module may be further divided into submodules with different tasks. One example of such a configuration is to divide it into *route planning*, *behavioral layer* and *motion planning* [4]. At the highest level of the planning module, the decision-making system of the vehicle determines a route through the road network to its requested destination. The task of the behavioral layer is to navigate the surrounding environment, determine the actions of other agents in traffic and decide on an appropriate driving behavior. Finally, the goal of the motion planner is to generate a local reference trajectory for the controller to follow. The trajectory should fulfill high-level goals specified from the preceding layers, avoid collision with surrounding obstacles and be feasible to execute.

The task of the perception module is to continuously scan and monitor the internal and external environment of an autonomous vehicle [26]. The stream of observations are generated by gathering information of the on-board sensors, such as radars, LIDARs, cameras, GNSS units and vehicle odometry [4]. Additionally, state-estimation is performed by fusing the sensor information together with prediction models of the vehicle. It is needed as all the important vehicle states are seldom directly available from sensor signals. Localization and mapping information as well as the state estimates are then used by the planner and controller.

The controller receives a reference trajectory from the planning module to follow. Together with information of the vehicle states, the controller can determine the required control signals which should be sent to the actuators in the vehicle. The controller may be decoupled into *lateral* and *longitudinal* control. Longitudinal control involves regulating the vehicle speed by determining the appropriate throttle command. On the contrary, lateral control is concerned with automatic steering of the vehicle to follow the reference. The underlying goal of the controller is to make the vehicle follow the trajectory while demonstrating desirable behaviors, such as keeping proper spacing to other vehicles and maintaining passenger comfort.

In planning and control, a trajectory is a generalization of a path. Since this thesis is only concerned with lateral control, the trajectory-following problem is collapsed into a path-following problem. This is done by assuming a constant velocity throughout the investigated scenarios. Furthermore, the function of the planning module is replaced by generating pre-defined paths. The paths considered are further explained

in Section 1.4.3. The vehicle module in Figure 1.1 is omitted in this brief overview and instead detailed Section 1.4.2.

1.4.1 Simulation environment

Testing aggressive maneuvering with live testing, is time consuming and expensive. Therefore, evaluating the system in simulation is an important and common step in the development process. The simulation environment that is used in this thesis is the commercial TruckMaker vehicle simulator seen in Figure 1.2. TruckMaker is a product developed by IPG Automotive and is a complete software solution that provides tools for simulation of heavy-duty vehicles using realistic high fidelity models and a modifiable environment.

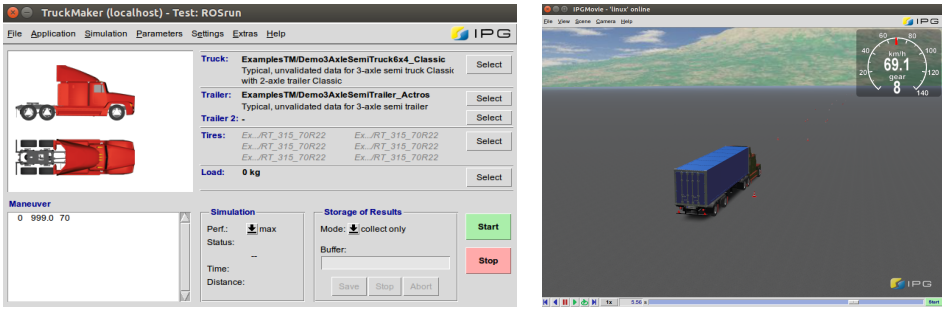

(a) TruckMaker main GUI.

(b) IPG Movie.

Figure 1.2: Overview of IPG TruckMaker.

1.4.2 Vehicle specification

The tractor and trailer combination used throughout this work is a model from the TruckMaker simulation environment. It is both used for the system identification and for simulation. The model consists of a conventional three-axle tractor, together with a two-axle semitrailer. The tractor and trailer are connected by a fifth-wheel hitch coupling. The fifth-wheel coupling limits roll and pitch motion of the trailer relative to the tractor but allows for free yaw rotational motion [28]. An overview of the vehicle can be seen in Figure 1.3.

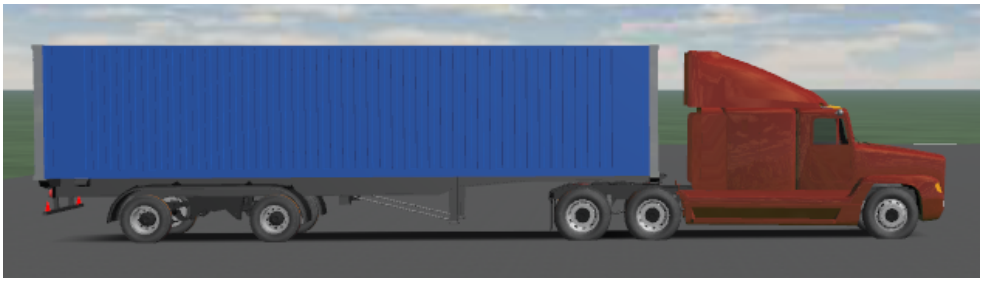

Figure 1.3: The tractor-trailer vehicle investigated.

1.4.3 Maneuver overview

For system identification and controller evaluation, the maneuvers of interest need to be defined. The baseline maneuver of this thesis work is a double lane change. This driving scenario requires the vehicle to switch lanes at high speeds while avoiding possible obstacles in the way. A schematic illustration of a double lane change maneuver is illustrated in Figure 1.4. The maneuver is chosen for its reproducibility and its relevancy to the considered problem. Since it is also a good representation of a possible emergency maneuver, the results found might be applicable to real driving situations. Finally, lane changing maneuvers are widely used in research for evaluation of both model and controller performance, see for example [16, 14, 5, 17, 19]. More detailed specifications of the created paths are later presented in Section 4.2.2.

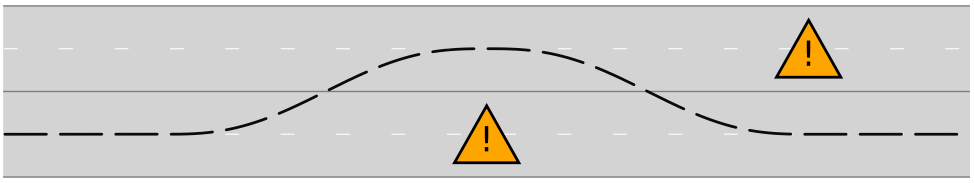

Figure 1.4: A double lane change scenario, illustrating an evasive maneuver.

2 Modeling and system identification

This chapter introduces several physical models of the lateral dynamics of the tractor-trailer system, as well as the system identification techniques used to estimate the model parameters.

2.1 Models

Several types of models are investigated in this work, which can be separated into two categories: kinematic and dynamic models. Kinematic models are derived based on kinematic constraints, i.e. the wheels can only move in the direction they point. On the contrary, dynamic models are derived from Newton's laws related to force and torque equilibriums of the system. All models are single-track bicycle models, which replace the left and right wheels of an axle with a single wheel [29].

Two different kinematic models are presented, one that just models the tractor, and one that also models the semitrailer. Three dynamic models of increasing complexity are also introduced. These include a tractor model, a tractor-trailer model, and a tractor-trailer model that also models roll effects. For the dynamic models, linear and nonlinear tire models are presented in Section 2.1.6.

2.1.1 Kinematic tractor model

The kinematic bicycle model is one of the simplest models of a tractor system. It is widely used in the control literature and has been shown to describe car-like vehicles well during normal driving situations [5, 18, 4, 27]. In [5] a kinematic and dynamic model is compared and it is concluded that a kinematic model describes the system sufficiently well during highway driving.

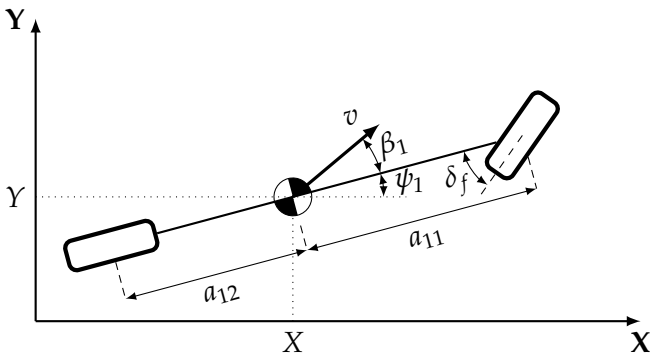

Figure 2.1: A kinematic bicycle model of a tractor system.

From the vehicle in Figure 2.1 a kinematic model is derived from assuming no-slip conditions of the front and rear wheels, resulting in the following differential equations [18]:

$$\dot{X} = v\cos(\psi_1 + \beta_1) \tag{2.1a}$$

$$\dot{Y} = v\sin(\psi_1 + \beta_1) \tag{2.1b}$$

$$\dot{\psi}_1 = v\frac{\sin\beta_1}{a_{12}} \tag{2.1c}$$

$$\beta_1 = \arctan\left(\frac{a_{12}}{a_{11}+a_{12}}\tan\delta_f\right) \tag{2.1d}$$

where the variables and parameters are described in Table 2.1.

Table 2.1: The variables and parameters for the kinematic models.

Symbol	Description
X	x-coordinate of tractor COM
Y	y-coordinate of tractor COM
ψ_1	Yaw angle of tractor
ψ_2	Yaw angle of trailer
δ_f	Steering angle of front wheels
v	Velocity of tractor
β_1	Side slip angle of tractor
a_{11}	Distance between COM and front axle for the tractor
a_{12}	Distance between COM and rear axle for the tractor
a_{21}	Distance between COM and the axle for the trailer
b_1	Distance between COM and the hitch point for the tractor
b_2	Distance between COM and the hitch point for the trailer

2.1.2 Kinematic tractor-trailer model

The kinematic tractor model can be extended to have an arbitrary number of trailers. Kinematic trailer models are used in literature for both planning and control [10, 9]. In [7] a recursive formula for a general n-trailer kinematic model is derived. This

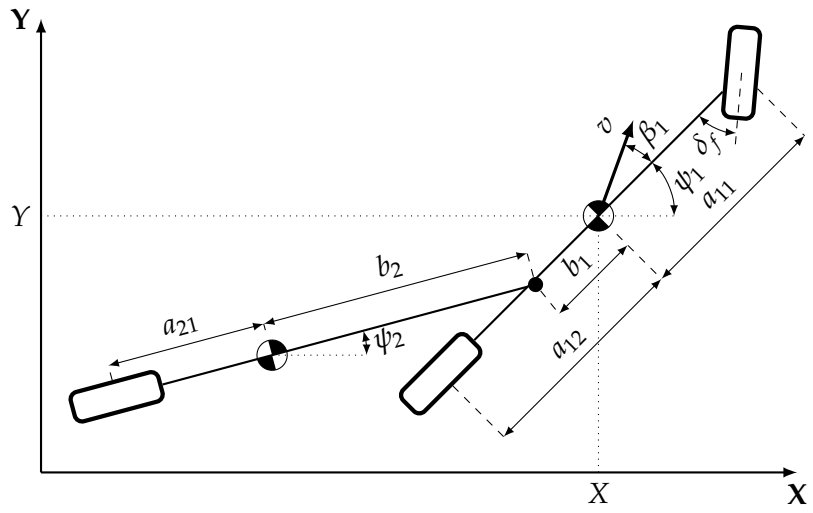

Figure 2.2: A kinematic bicycle model of a tractor-semitrailer system.

model describes a kinematic tractor-trailer system with off-hitching, i.e. when the hitch joint and rear axle are offset longitudinally. Using the recursive formula in [7] for a tractor-trailer vehicle (see Figure 2.2), the following nonlinear model is obtained:

$$\dot{X} = v\cos(\psi_1 + \beta_1) \tag{2.2a}$$
$$\dot{Y} = v\sin(\psi_1 + \beta_1) \tag{2.2b}$$
$$\dot{\psi}_1 = v\frac{\sin\beta_1}{a_{12}} \tag{2.2c}$$
$$\dot{\psi}_2 = v\frac{\sin(\psi_1 - \psi_2)}{b_2 + a_{21}} - v\frac{(b_1 - a_{12})\cos(\psi_1 - \psi_2)\sin\beta_1}{a_{12}(b_2 + a_{21})} \tag{2.2d}$$
$$\beta_1 = \arctan\left(\frac{a_{12}}{a_{11} + a_{12}}\tan\delta_f\right) \tag{2.2e}$$

where the variables and parameters are described in Table 2.1.

2.1.3 Dynamic tractor model

During more aggressive maneuvers, models that take dynamic effects into account are needed to accurately describe the system [18, 27]. They have been used to successfully control car-like vehicles at the limits of handling [30, 31]. A dynamic bicycle model can be derived from a force and torque equilibrium of the vehicle in Figure 2.3. This results in the following dynamic model:

$$\dot{X} = v_x\cos\psi_1 - v_y\sin\psi_1 \tag{2.3a}$$
$$\dot{Y} = v_x\sin\psi_1 + v_y\cos\psi_1 \tag{2.3b}$$
$$\dot{\psi}_1 = \dot{\psi}_1 \tag{2.3c}$$
$$\ddot{\psi}_1 = \frac{1}{I_{zz,1}}\left(a_{11}F_{y,f}\cos\delta_f - a_{12}F_{y,r}\right) \tag{2.3d}$$
$$\dot{v}_y = -v_x\dot{\psi}_1 + \frac{1}{m_1}\left(F_{y,f}\cos\delta_f + F_{y,r}\right) \tag{2.3e}$$

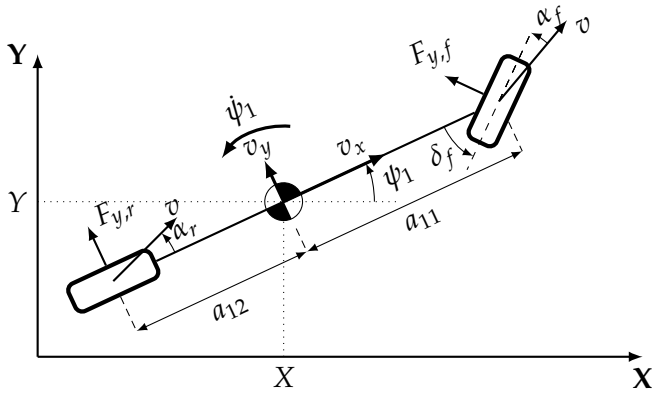

Figure 2.3: A dynamic bicycle model of a tractor system.

where the variables and parameters are described in Table 2.2. In this model the lateral tire forces $F_{y,i}$ are functions of the lateral slip. This relation is the tire model, which is further described in Section 2.1.6.

Table 2.2: The variables and parameters for the dynamic models.

Symbol	Description
X	x-coordinate of tractor COM
Y	y-coordinate of tractor COM
ψ_1	Yaw angle of tractor
ψ_2	Yaw angle of trailer
v_x	Longitudinal velocity of tractor
v_y	Lateral velocity of tractor
δ_f	Steering angle of front wheels
m_1	Mass of tractor
m_2	Mass of trailer
$I_{zz,1}$	Yaw moment of inertia of tractor
$I_{zz,2}$	Yaw moment of inertia of trailer
a_{11}	Distance between COM and front axle for the tractor
a_{12}	Distance between COM and rear axle for the tractor
a_{21}	Distance between COM and the axle for the trailer
b_1	Distance between COM and the hitch point for the tractor
b_2	Distance between COM and the hitch point for the trailer
$F_{y,f}$	Lateral force of front tractor tires
$F_{y,r}$	Lateral force of rear tractor tires
$F_{y,t}$	Lateral force of trailer tires

2.1.4 Dynamic tractor-trailer model

The dynamic tractor model can be extended to include a trailer. Dynamic trailer models are frequently used for analyzing the handling characteristics of tractor-trailer vehicles [11, 29]. They are also used for braking and steering control of tractor-trailer vehicles during emergency braking [25]. In [16], several dynamic tractor-trailer models

from the literature are compared. One of the better performing models is presented below. This model assumes that the longitudinal velocity of the trailer is equivalent with the tractor and that the hitch angle is small.

$$\dot{X} = v_x \cos\psi_1 - v_y \sin\psi_1 \tag{2.4a}$$
$$\dot{Y} = v_x \sin\psi_1 + v_y \cos\psi_1 \tag{2.4b}$$
$$\dot{q} = \dot{q} \tag{2.4c}$$
$$\begin{bmatrix}\dot{v}_y & \ddot{q}^T\end{bmatrix}^T = M_\psi^{-1} H_\psi(q, \dot{q}, v_x, v_y, F_y) \tag{2.4d}$$

where $q = \begin{bmatrix}\psi_1 & \psi_2\end{bmatrix}^T$, $F_y = \begin{bmatrix}F_{y,f} & F_{y,r} & F_{y,t}\end{bmatrix}^T$, and

$$M_\psi = \begin{bmatrix} m_1 + m_2 & -b_1 m_2 & -b_2 m_2 \\ -b_1 m_2 & I_{zz,1} + b_1^2 m_2 & b_1 b_2 m_2 \\ -b_2 m_2 & b_1 b_2 m_2 & I_{zz,2} + b_2^2 m_2 \end{bmatrix} \tag{2.5a}$$
$$H_\psi(q, \dot{q}, v_x, v_y, F_y) = \begin{bmatrix} F_{y,f} + F_{y,r} + F_{y,t} - m_1 \dot{\psi}_1 v_x - m_2 \dot{\psi}_1 v_x \\ F_{y,f} a_{11} - F_{y,r} a_{12} - F_{y,t} b_1 + b_1 m_2 \dot{\psi}_1 v_x \\ -F_{y,t} a_{21} - F_{y,t} b_2 + b_2 m_2 \dot{\psi}_1 v_x \end{bmatrix} \tag{2.5b}$$

where M_ψ is assumed to be invertible. The variables and parameters in these differential equations are described in Table 2.2.

2.1.5 Dynamic tractor-trailer roll model

As the risk of rollover is high during aggressive maneuvering with heavy vehicles [21, 32, 28], a model that includes rolling phenomena of the tractor and semitrailer is developed. Roll models of tractor-trailer vehicles are frequently used in literature for active roll control systems [21, 15, 33]. In [21], a general method is derived for construction of dynamic tractor-trailer roll models with an arbitrary number of trailers. The method models the roll dynamics by adding a sprung mass connected to the axles with a rotational spring and damper, which can rotate about a fixed longitudinal axis, see Figure 2.4. This is done for both the tractor and trailer. The connection between the two sprung bodies is then modeled as a rotational spring in the hitch joint.

The model created with their method also models the suspension dynamics of the tires separately from the rest of the suspension. This phenomenon and the effect of the coupling force on the roll dynamics is neglected, which results in the following differential equations:

$$\dot{X} = v_x \cos\psi_1 - v_y \sin\psi_1 \tag{2.6a}$$
$$\dot{Y} = v_x \sin\psi_1 + v_y \cos\psi_1 \tag{2.6b}$$
$$\dot{q} = \dot{q} \tag{2.6c}$$
$$\begin{bmatrix}\dot{v}_y & \ddot{q}^T\end{bmatrix}^T = M_\phi^{-1} H_\phi(q, \dot{q}, v_x, v_y, F_y) \tag{2.6d}$$

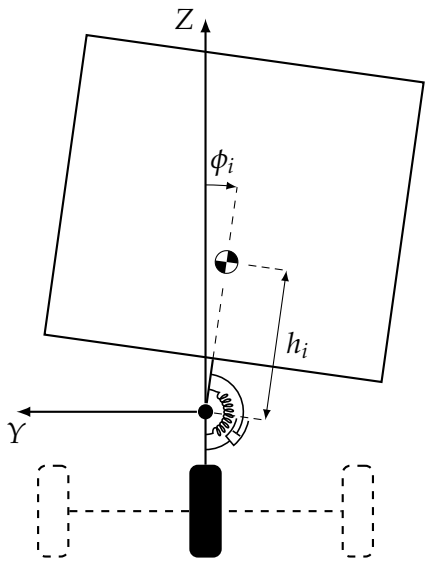

Figure 2.4: Rear view of ith body in roll model, where $i = 1$ is the tractor, and $i = 2$ is the trailer.

where $q = \begin{bmatrix} \psi_1 & \psi_2 & \phi_1 & \phi_2 \end{bmatrix}^T$, $F_y = \begin{bmatrix} F_{y,f} & F_{y,r} & F_{y,t} \end{bmatrix}^T$, and

$$M_\phi = \begin{bmatrix} m_1 + m_2 & -b_1 m_2 & -b_2 m_2 & -h_1 m_{s,1} & -h_2 m_{s,2} \\ -b_1 m_2 & I_{zz,1} + b_1^2 m_2 & b_1 b_2 m_2 & 0 & b_1 h_2 m_{s,2} \\ -b_2 m_2 & b_1 b_2 m_2 & I_{zz,2} + b_2^2 m_2 & 0 & b_2 h_2 m_{s,2} \\ 0 & 0 & 0 & I_{xx,1} & 0 \\ 0 & 0 & 0 & 0 & I_{xx,2} \end{bmatrix} \tag{2.7a}$$

$$H_\phi(q, \dot{q}, v_x, v_y, F_y) = \begin{bmatrix} F_{y,f} + F_{y,r} + F_{y,t} - \dot{\psi}_1 m_1 v_x - \dot{\psi}_1 m_2 v_x \\ F_{y,f} a_{11} + F_{y,r} a_{12} - F_{y,t} b_1 + \dot{\psi}_1 b_1 m_2 v_x \\ F_{y,t} a_{21} - F_{y,t} b_2 + \dot{\psi}_1 b_2 m_2 v_x \\ \dot{\psi}_1 h_1 m_{s,1} v_x + g h_1 m_{s,1} \psi_1 - k_1 \psi_1 - \dot{\phi}_1 d_1 - k_\phi(\psi_1 - \psi_2) \\ \dot{\psi}_2 h_2 m_{s,2} v_x + g h_2 m_{s,2} \psi_2 - k_2 \psi_2 - \dot{\phi}_2 d_2 + k_\phi(\psi_1 - \psi_2) \end{bmatrix} \tag{2.7b}$$

where the mass matrix, M_ϕ is assumed to be invertible. All parameters and variables are described in Tables 2.2 and 2.3.

This model assumes that the spring and damper are linear for both the tractor and trailer. This is a reasonable assumption for small roll angles as the effect of nonlinearities is typically small. However, when the suspension is close to bottoming out this assumption becomes inaccurate [21].

Table 2.3: The variables and parameters added for the roll model.

Symbol	Description
ϕ_1	Roll angle of tractor
ϕ_2	Roll angle of trailer
$m_{s,1}$	Sprung mass of tractor
$m_{s,2}$	Sprung mass of trailer
$I_{xx,1}$	Roll moment of inertia of sprung tractor mass
$I_{xx,2}$	Roll moment of inertia of sprung trailer mass
h_1	Height of COM over the roll center for the trailer
h_2	Height of COM over the roll center for the trailer
k_1	Roll stiffness of tractor
k_2	Roll stiffness of trailer
k_ϕ	Roll stiffness of hitch joint
d_1	Roll damping of tractor
d_2	Roll damping of trailer

2.1.6 Tire models

Many different tire models exist to describe the interaction between tire and road [34]. In this thesis the tire model refers to the cornering force-slip angle relationship of a tire. Lateral tire slip is defined as the angle between the velocity vector of the tire and the direction of the tire. For the tractor-trailer system this can be written as [35]:

$$\alpha_f = \arctan\left(\frac{v_y + a_{11}\dot{\psi}_1}{v_x}\right) - \delta_f \tag{2.8a}$$

$$\alpha_r = \arctan\left(\frac{v_y - a_{12}\dot{\psi}_1}{v_x}\right) \tag{2.8b}$$

$$\alpha_t = \arctan\left(\frac{\left(v_y - b_1\dot{\psi}_1\right)\cos\left(\psi_1 - \psi_2\right) - \dot{\psi}_2(b_2 + a_{21}) + v_x \sin\left(\psi_1 - \psi_2\right)}{v_x \cos\left(\psi_1 - \psi_2\right) - \left(v_y - b_1\dot{\psi}_1\right)\sin\left(\psi_1 - \psi_2\right)}\right) \tag{2.8c}$$

These relations can be simplified by assuming that the slip, steering, and hitch angles are small and that the longitudinal velocities of the tractor and trailer are the same. By doing this, Equation (2.8) are converted to the following:

$$\alpha_f = \frac{v_y + a_{11}\dot{\psi}_1}{v_x} - \delta_f \tag{2.9a}$$

$$\alpha_r = \frac{v_y - a_{12}\dot{\psi}_1}{v_x} \tag{2.9b}$$

$$\alpha_t = \frac{v_y - b_1\dot{\psi}_1 - \dot{\psi}_2(b_2 + a_{21})}{v_x} + \psi_1 - \psi_2 \tag{2.9c}$$

which are linear in the modeled states and the steering angle. For a realistic vehicle model, the steering angle, δ_f is limited by the mechanical system and the actuators. These limitations are expressed as:

$$|\delta_f| \leqslant 45^\circ \tag{2.10a}$$

$$|\dot{\delta}_f| \leqslant 45\,^\circ/\mathrm{s} \tag{2.10b}$$

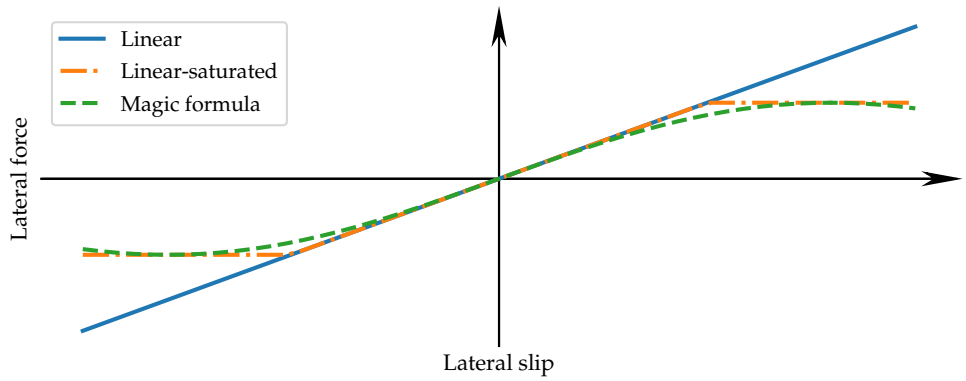

Figure 2.5: The general behavior of a linear, linear-saturated, and Pacejka's tire model.

A common tire model is the linear model [29], defined as:

$$F_{y,i} = -C_{\alpha,i}\alpha_i, \qquad i \in \{f, r, t\} \tag{2.11}$$

where the lateral tire force is linearly dependent on the lateral tire slip. This model is typically a good approximation for small slip angles when the operating point is far from the limit of traction. This is often the case for tractor-trailer systems as their cornering performance is more limited by the dynamic behavior of the trailer than friction. Additionally, truck tires tend to be more linear than car tires [12].

To describe the tire behavior for larger slip angles, nonlinear tire models must be used. A common nonlinear tire model is the empirical Pacejka's Magic Formula model. This model adds two additional features to the linear model, a saturation where the lateral force reaches its peak, and a decline after the peak to model the friction force from sliding friction [29]. The Magic Formula model is:

$$F_{y,i} = D \sin\left(C \arctan\left(B\alpha_i - E\left(B\alpha_i - \arctan(B\alpha_i)\right)\right)\right), \qquad i \in \{f, r, t\} \tag{2.12}$$

This model uses three more parameters than the linear model. A simpler alternative to the Magic Formula is to use a piecewise linear model with a linear region for slip angles around zero, and a saturation for larger angles. This is the same as using a simple brush model with the same friction coefficient for static and sliding friction [29], and can be written as:

$$F_{y,i} = \begin{cases} -C_{\alpha,i}\alpha_i, & \text{if } -F_{y,i,max} \leqslant -C_{\alpha,i}\alpha_i \leqslant F_{y,i,max} \\ -F_{y,i,max} \operatorname{sign} \alpha_i, & \text{otherwise} \end{cases}, \qquad i \in \{f, r, t\} \tag{2.13}$$

This model only adds the maximum lateral force parameter in addition to the cornering stiffness. It is because of this simplicity that this model is used. One issue with this model is that it has discontinuous derivatives, which can be problematic during optimization. This can be resolved by implementing the saturation with a smooth maximum function, e.g. a LogSumExp function. Figure 2.5, shows the general behavior of this model together with a linear model and the Magic Formula.

2.2 System identification

The parameters in the models described in Section 2.1 have to be identified before the models can be used. In this work, this is done in two different ways, by directly using parameters from the TruckMaker model and by identifying them from data. The parameters that are directly identified are the inertias of both the tractor and the trailer. These would also be reasonably easy to measure and approximate on a physical tractor-trailer. Similarly, other parameters such as axle locations and the center of gravity would be easy to measure on a real truck. They are, however, allowed to differ from their measured values to improve model fit. This is possible as the models are only approximations of the system, and their maximum performance does not necessarily occur when the parameters are the same as the true parameter value.

The model structure might make it impossible to uniquely identify certain parameters simultaneously. For example, in the dynamic tractor model in Section 2.1.3, the yaw inertia, mass, and cornering stiffnesses cannot all be identified. This can be seen because if all four parameters are scaled by the same factor k, the resulting model will not change. This is discussed in [36] for the identification of a dynamic car model using only stationary maneuvers.

The problem with identifiability partly explains why the inertias are fixed. Another reason is that identifying many parameters in the mass matrix in the dynamic trailer models in Sections 2.1.4 and 2.1.5 makes the implementation slow, likely due to slow automatic differentiation of the matrix inversion.

2.2.1 Optimization problem

To identify the parameters, a nonlinear optimization problem is formulated. It is assumed that perfect measurements of all states are available. The problem is then constructed to minimize the squared prediction error of a one-step predictor. The one-step predictor is created by simulating the system forward one step, using an Euler forward discretization of the continuous model.

$$\hat{x}_{k+1} = x_k + f(x_k, u_k, \theta)dt \tag{2.14}$$

where f is the continuous model of the system, defined as $\dot{x} = f(x, u, \theta)$, dt is the time step, and θ is the parameter vector. The time step is selected to be equal to the sampling time of the dataset. From this, the optimization problem is defined as follows:

$$\min_{\theta} \sum_{k=1}^{n-1} \|x_{k+1} - x_k - f(x_k, u_k)dt\|_W^2 \tag{2.15}$$

where n is the size of the dataset, and $\| \ \|_W^2$ denotes the weighted l_2-norm with the weight matrix W. This matrix determines how much the prediction error of each state should be weighted. As the optimization problem is nonlinear, there is no guarantee that the solution is the global optimum. It is therefore important that the parameter vector is initialized well. Additionally, constraints are added to the parameters to help the optimizer converge to a good minimum, with a low cost. These included requiring all parameters to be positive, and constraints that reflect prior knowledge of the system. For example, requiring that the roll stiffness and damping coefficients for the trailer are larger than for the tractor.

The reason that the one-step ahead prediction error is minimized is to keep the problem simple and make it computationally cheap. An alternative formulation would be to predict the system several time steps forward, and minimize the prediction error there. One advantage of that approach is that the prediction of important states such as position and heading angle can directly be optimized. This is not done as the simpler approach results in similar model performance while being much faster.

Another method of identifying the parameter values is to estimate them online. This can for example, be done using moving horizon estimation, where the deviation of the model from a finite horizon of measurements is minimized. This has been used for parameter and state estimation in autonomous systems [37, 38]. Estimating the parameters online are beneficial if the parameters change over time, e.g. if different trailers are used or if the environment changes.

3 Lateral control techniques

This chapter presents different control techniques for lateral control of tractor-trailer vehicles. By controlling the steering angle of the front wheels, the objective of the lateral controller is to safely follow a path and keep the deviation from the path small. First an error model of the system is presented, which is used in the remainder of the thesis. Then linear-quadratic (LQ) control and model predictive control (MPC) are introduced.

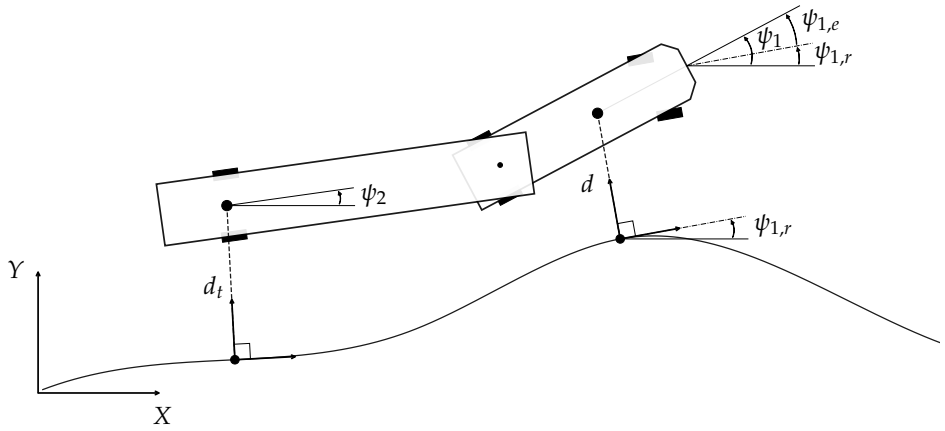

Figure 3.1: Frenet-Serret frame of a tractor-trailer system.

3.1 Error models

For lateral control of a vehicle it is natural to represent the vehicle coordinates in a Frenet-Serret frame as opposed to Cartesian coordinates. The Frenet-Serret frame is a path coordinate system that represents the vehicle's position as a progression along a path, $s(t)$ as well as its signed lateral distance to the path, $d(t)$, see Figure 3.1. The orientation of the tractor can also be represented relative to the path with $\psi_{1,e} = \psi_1 - \psi_{1,r}$.

In this representation an error model can be derived that describes how the path relative coordinates change over time. An error model is especially useful in the creation of an LQ controller, because the goal in the LQ optimization problem intro-

duced in (3.27) is to move all states to the origin. The error models for the models in Section 2.1 are presented below.

3.1.1 Kinematic tractor

In [39] an error model is created for a kinematic vehicle model. This transforms the model in Equation (2.1) to the following:

$$\dot{x}_e = \begin{bmatrix} \dot{d} \\ \dot{\psi}_{1,e} \end{bmatrix} = \begin{bmatrix} v \sin(\psi_{1,e} + \beta_1) \\ \dot{\psi}_1 - \dot{s}c(s) \end{bmatrix} \tag{3.1}$$

where $c(s)$ is the curvature of the path. The velocity along the path, $\dot{s}$ is given by:

$$\dot{s} = \frac{v \cos(\psi_{1,e} + \beta_1)}{1 - dc(s)} \tag{3.2}$$

which is further assumed to be $\dot{s} = v$ to simplify the model. This assumption is valid when $\psi_{1,e} + \beta_1$ and $dc(s)$ are close to zero. The expression for the yaw rate of the tractor, $\dot{\psi}_1$ is found in Equation (2.1). Inserting it together with the simplified $\dot{s}$ into Equation (3.1) yields:

$$\dot{x}_e = \begin{bmatrix} v \sin(\psi_{1,e} + \beta_1) \\ \frac{v}{a_{12}} \sin(\beta_1) - vc(s) \end{bmatrix} \tag{3.3}$$

where the sideslip of the tractor, β_1 is given by:

$$\beta_1 = \arctan\left(\frac{a_{12}}{a_{11} + a_{12}} \tan \delta_f \right) \tag{3.4}$$

3.1.2 Kinematic trailer

Using the kinematic trailer model presented in Section 2.1.2, an error model is derived. The kinematic trailer model can be transformed in the same way as was done in the previous section for the kinematic tractor model. In addition to the error states found in the previous section, an additional state must be added to represent the error in the hitch angle, Γ_e. This results in the following error model for the kinematic trailer:

$$\dot{x}_e = \begin{bmatrix} \dot{d} \\ \dot{\psi}_{1,e} \\ \dot{\Gamma}_e \end{bmatrix} = \begin{bmatrix} v \sin(\psi_{1,e} + \beta_1) \\ \dot{\psi}_1 - \dot{s}c(s) \\ \dot{\Gamma} - \dot{\Gamma}_r \end{bmatrix} \tag{3.5}$$

where Γ denotes the hitch angle, which is given by:

$$\Gamma = \psi_1 - \psi_2 \tag{3.6}$$

Furthermore, Γ_r denotes the hitch angle reference and a definition of it is given in Section 3.1.6. The tractor and trailer yaw rates, $\dot{\psi}_1$ and $\dot{\psi}_2$, are found in Equation (2.2). These expressions, together with the simplified $\dot{s}$ from Section 3.1.1 are inserted into (3.5). The full error model is then given by:

$$\dot{x}_e = \begin{bmatrix} v \sin(\psi_{1,e} + \beta_1) \\ \frac{v}{a_{12}} \sin(\beta_1) - vc(s) \\ v\left(\frac{\sin\beta_1}{a_{12}} - \frac{\sin(\Gamma_e + \Gamma_r)}{b_2 + a_{21}} + \frac{(b_1 - a_{12})\cos(\Gamma_e + \Gamma_r)\sin\beta_1}{a_{12}(b_2 + a_{21})} \right) - \dot{\Gamma}_r \end{bmatrix} \tag{3.7}$$

where the sideslip of the tractor, β_1 is given by (3.4).

3.1.3 Dynamic tractor

Using the dynamic tractor model in Section 2.1.3 an error model is derived. In the same manner as the kinematic models, an error model for vehicles with separate longitudinal and lateral velocities, such as the dynamic models, is derived in [40]. This results in the following Frenet-Serret representation:

$$\dot{d} = v_x \sin\psi_{1,e} + v_y \cos\psi_{1,e} \tag{3.8a}$$
$$\dot{\psi}_{1,e} = \dot{\psi}_1 - \dot{s}c(s) \tag{3.8b}$$

By differentiating these equations, the dynamic tractor model in Equation (2.3) can be transformed to an error model:

$$\dot{x}_e = \begin{bmatrix} \dot{z} \\ \ddot{z} \end{bmatrix} \tag{3.9}$$

where:

$$\dot{z} = \begin{bmatrix} \dot{d} & \dot{\psi}_{1,e} \end{bmatrix}^T \tag{3.10a}$$
$$\ddot{z} = \begin{bmatrix} (\dot{v}_x - v_y\dot{\psi}_{1,e})\sin\psi_{1,e} + (\dot{v}_y + v_x\dot{\psi}_{1,e})\cos\psi_{1,e} \\ \ddot{\psi}_1 - \ddot{s}c(s) - \dot{s}^2\frac{\mathrm{d}}{\mathrm{d}s}c(s) \end{bmatrix} \tag{3.10b}$$

The velocity, $\dot{s}$ and acceleration, $\ddot{s}$ along the path are given by:

$$\dot{s} = \frac{v_x\cos\psi_{1,e} - v_y\sin\psi_{1,e}}{1 - dc(s)} \tag{3.11a}$$

$$\ddot{s} = \frac{\dot{\psi}_{1,e}v_x\sin(\psi_{1,e}) + \dot{\psi}_{1,e}v_y\cos(\psi_{1,e}) - \dot{v}_x\cos(\psi_{1,e}) + \dot{v}_y\sin(\psi_{1,e})}{(c(s)d-1)} + \frac{\left(\dot{d}c(s) + \dot{s}d\frac{\mathrm{d}}{\mathrm{d}s}c(s)\right)\left(v_x\cos(\psi_{1,e}) - v_y\sin(\psi_{1,e})\right)}{(c(s)d-1)^2} \tag{3.11b}$$

Similarly to the kinematic error models, $\dot{s}$ is assumed to be equal to v_x. Additionally the longitudinal speed is assumed to be constant, which results in $\ddot{s} = \dot{v}_x = 0$. With these assumptions together with $\dot{v}_y$, and $\ddot{\psi}_1$ from (2.3), as well as v_y from (3.8a), $\ddot{z}$ becomes:

$$\ddot{z} = \begin{bmatrix} (v_x\sin\psi_{1,e} - \dot{d})\dot{\psi}_{1,e}\tan\psi_{1,e} + (\frac{1}{m_1}\left(F_{y,f}\cos\delta_f + F_{y,r}\right) - v_x\dot{\psi}_{1,r})\cos\psi_{1,e} \\ \frac{1}{I_{zz,1}}\left(a_{11}F_{y,f}\cos\delta_f - a_{12}F_{y,r}\right) - \dot{s}^2\frac{\mathrm{d}}{\mathrm{d}s}c(s) \end{bmatrix} \tag{3.12}$$

3.1.4 Dynamic tractor-trailer

Using the dynamic tractor-trailer model in Section 2.1.4 an error model is derived. This is done using the same procedure as for the dynamic tractor model. Similarly to Section 3.1.2, the hitch angle error has to be added, which results in:

$$\dot{x}_e = \begin{bmatrix} \dot{z} \\ \ddot{z} \end{bmatrix} \tag{3.13}$$

where:

$$\dot{z} = \begin{bmatrix} \dot{d} & \dot{\psi}_{1,e} & \dot{\Gamma}_e \end{bmatrix}^T \tag{3.14a}$$

$$\ddot{z} = \begin{bmatrix} (\dot{v}_x - v_y\dot{\psi}_{1,e})\sin\psi_{1,e} + (\dot{v}_y + v_x\dot{\psi}_{1,e})\cos\psi_{1,e} \\ \ddot{\psi}_1 - \ddot{s}c(s) - \dot{s}^2\frac{\mathrm{d}}{\mathrm{d}s}c(s) \\ \ddot{\Gamma} - \ddot{\Gamma}_r \end{bmatrix} \tag{3.14b}$$

The expressions for $\dot{v}_y$, $\ddot{\psi}_1$, and $\ddot{\psi}_2$ are found in (2.4) and v_y is found in (3.8a). This together with the simplified $\dot{s}$, and $\ddot{s}$ results in the following expression:

$$\ddot{z} = \begin{bmatrix} (v_x\sin\psi_{1,e} - \dot{d})\dot{\psi}_{1,e}\tan\psi_{1,e} + ((M_\psi^{-1}\tilde{H}_\psi)_1 + v_x\dot{\psi}_{1,e})\cos\psi_{1,e} \\ (M_\psi^{-1}\tilde{H}_\psi)_2 - \dot{s}^2\frac{\mathrm{d}}{\mathrm{d}s}c(s) \\ (M_\psi^{-1}\tilde{H}_\psi)_2 - (M_\psi^{-1}\tilde{H}_\psi)_3 - \ddot{\Gamma}_r \end{bmatrix} \tag{3.15}$$

where the notation $(\mathbf{a})_i$ denotes the i:th element of the vector $\mathbf{a}$ and $\tilde{H}_\psi$ is an alias for:

$$\tilde{H}_\psi = H_\psi\left(q, \dot{q}, v_x, \frac{\dot{d} - v_x\sin\psi_{1,e}}{\cos\psi_{1,e}}, F_y\right) \tag{3.16}$$

where:

$$q = \begin{bmatrix} \psi_{1,e} + \psi_{1,r} & \psi_{1,e} + \psi_{1,r} - \Gamma_e - \Gamma_r \end{bmatrix}^T \tag{3.17a}$$

$$\dot{q} = \begin{bmatrix} \dot{\psi}_{1,e} + v_x c(s) & \dot{\psi}_{1,e} + v_x c(s) - \dot{\Gamma}_e + \dot{\Gamma}_r \end{bmatrix}^T \tag{3.17b}$$

from Section 2.1.4.

3.1.5 Dynamic tractor-trailer roll

The error model of the dynamic trailer is naturally extended to include roll. This is done by adding an error state for the tractor and trailer roll angles and rates, $\phi_{1,e}$ and $\phi_{2,e}$

$$\dot{x}_e = \begin{bmatrix} \dot{z} \\ \ddot{z} \end{bmatrix} \tag{3.18}$$

where:

$$\dot{z} = \begin{bmatrix} \dot{d} & \dot{\psi}_{1,e} & \dot{\Gamma}_e & \dot{\phi}_{1,e} & \dot{\phi}_{2,e} \end{bmatrix}^T \tag{3.19a}$$

$$\ddot{z} = \begin{bmatrix} (\dot{v}_x - v_y\dot{\psi}_{1,e})\sin\psi_{1,e} + (\dot{v}_y + v_x\dot{\psi}_{1,e})\cos\psi_{1,e} \\ \ddot{\psi}_1 - \ddot{s}c(s) - \dot{s}^2\frac{\mathrm{d}}{\mathrm{d}s}c(s) \\ \ddot{\Gamma} - \ddot{\Gamma}_r \\ \ddot{\phi}_1 - \ddot{\phi}_{1,r} \\ \ddot{\phi}_2 - \ddot{\phi}_{2,r} \end{bmatrix} \tag{3.19b}$$

The roll references $\ddot{\phi}_{1,r}$ and $\ddot{\phi}_{2,r}$ are further discussed in Section 3.1.6. The expressions for $\dot{v}_y$, $\ddot{\psi}_1$, $\ddot{\psi}_2$, $\ddot{\phi}_1$, and $\ddot{\phi}_2$ are found in (2.6) and v_y is found in (3.8a). This together with the simplified $\dot{s}$, and $\ddot{s}$ results in the following expression:

$$\ddot{z} = \begin{bmatrix} (v_x\sin\psi_{1,e} - \dot{d})\dot{\psi}_{1,e}\tan\psi_{1,e} + ((M_\phi^{-1}\tilde{H}_\phi)_1 + v_x\dot{\psi}_{1,e})\cos\psi_{1,e} \\ (M_\phi^{-1}\tilde{H}_\phi)_2 - \dot{s}^2\frac{\mathrm{d}}{\mathrm{d}s}c(s) \\ (M_\phi^{-1}\tilde{H}_\phi)_2 - (M_\phi^{-1}\tilde{H}_\phi)_3 - \ddot{\Gamma}_r \\ (M_\phi^{-1}\tilde{H}_\phi)_4 - \ddot{\phi}_{1,r} \\ (M_\phi^{-1}\tilde{H}_\phi)_5 - \ddot{\phi}_{2,r} \end{bmatrix} \tag{3.20}$$

where $\tilde{H}_\phi$ is an alias for:

$$\tilde{H}_\phi = H_\phi\left(q, \dot{q}, v_x, \frac{\dot{d} - v_x \sin\psi_{1,e}}{\cos\psi_{1,e}}, F_y\right) \tag{3.21}$$

where:

$$q = \begin{bmatrix}\psi_{1,e} + \psi_{1,r} & \psi_{1,e} + \psi_{1,r} - \Gamma_e - \Gamma_r & \psi_{1,e} + \psi_{1,r} & \phi_{2,e} + \phi_{2,r}\end{bmatrix}^T \tag{3.22a}$$

$$\dot{q} = \begin{bmatrix}\dot{\psi}_{1,e} + v_x c(s) & \dot{\psi}_{1,e} + v_x c(s) - \dot{\Gamma}_e + \dot{\Gamma}_r & \dot{\psi}_{1,e} + \dot{\psi}_{1,r} & \dot{\psi}_{2,e} + \dot{\psi}_{2,r}\end{bmatrix}^T \tag{3.22b}$$

from Section 2.1.5.

3.1.6 Trailer reference

When a trailer or roll model is used, up to six additional states are available: the hitch angle $\Gamma = \psi_1 - \psi_2$, the roll angle of the tractor ϕ_1, the roll angle of the trailer ϕ_2, as well as the rate of these states. There are many possibilities for how the controllers could use these states. The most simple approach would be to disregard them and only weight their effect on the tractor. However, this may not lead to satisfactory results, as the goal of the controller is not to only minimize the tractor errors, but to minimize the deviation from the reference for both the tractor and trailer.

One straightforward way to do this would be to instead control all trailer and roll states to zero. This approach is selected for the roll angles and rates, as minimizing all roll motion is desired. This means that $\ddot{\phi}_{1,r}$ and $\ddot{\phi}_{2,r}$ are set to zero in the error model. However, this is not the case with the hitch angle and rate, as this would not minimize the trailer deviation unless the reference is a straight line and the tractor errors are zero. In spite of this, it could still result in a low deviation as large trailer oscillations would be avoided.

These arguments motivate the need for a hitch angle reference that actually minimizes the deviation of the trailer. One problem with this is that no general closed-form expression for the trailer deviation exists [8]. In an MPC controller, this could be circumvented by numerically calculating the trailer deviation, and using finite differences to approximate its derivatives, which is done in [10] for a path planner. This is not used as it would make the optimization slower and because there is no direct equivalent for the LQ controller. Instead a hitch angle reference, Γ_r is calculated by finding the hitch angle that minimizes the trailer deviation when $\psi_{1,e} = 0$ and $d = 0$. This is done numerically for every point of the path.

The hitch reference is approximately related to the trailer cross-track error according to:

$$d_t \approx d - b_1 \sin\psi_{1,e} - (b_2 + a_{21}) \sin(\psi_{1,e} - \Gamma_e) \tag{3.23}$$

This relation approximates the cross-track error by projecting the position of the trailer on a straight line with the same slope as the tractor reference point. See Figure 3.2 for a visualization of this approximation.

The approximated cross-track error can be included in the LQ and MPC controllers by modifying the weight matrix Q, as done in [20]. Naturally, this can only be done for the trailer model, and is done as follows. First a new vector is defined with both the error states and the cross-track approximation:

$$z = \begin{bmatrix} x_e \\ d_t \end{bmatrix} \tag{3.24}$$

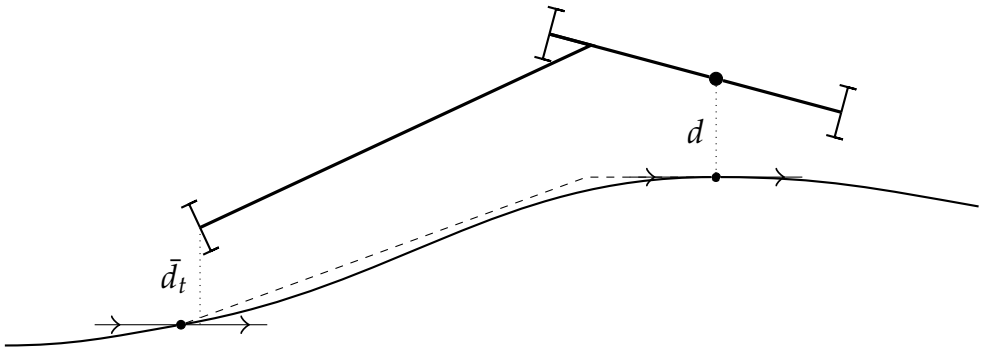

Figure 3.2: The approximated trailer cross-track error $\bar{d}_t$, shown together with the dashed reference position.

By linearizing Equation (3.23), this can then be written as linear function of the state vector.

$$z \approx \begin{bmatrix} I_n \\ \frac{\partial d_t}{\partial x_e}\Big|_{x_e=0} \end{bmatrix} x_e \triangleq M x_e \tag{3.25}$$

The relation between the weight matrix for z and x_e can then be written as:

$$z^T \overline{Q} z \approx x_e^T \underbrace{M^T \overline{Q} M}_{Q} x_e \tag{3.26}$$

where $\overline{Q}$ allows the semitrailer cross-track error in z to be weighted.

3.2 Linear-quadratic regulator

In this section the LQ controller is introduced. The control signal, $u(t)$ in the LQ controller consists of two parts, the feedforward u_0 and the state feedback $Kx(t)$. The purpose of the feedforward is to track the reference signal, while the feedback should compensate for modeling errors and other disturbances.

The feedback gain, K is calculated with LQ control, which is a method of optimally determining a linear state feedback control law for linear systems [41]. The time-invariant infinite horizon LQ control problem is:

$$\begin{aligned} \min_{u(t)} \quad & J = \int_0^\infty x(t)^T Q x(t) + u(t)^T R u(t) dt \\ \text{s.t.} \quad & \dot{x}(t) = Ax(t) + Bu(t) \\ & x(0) = x_0 \end{aligned} \tag{3.27}$$

The solution to this problem is a linear state feedback controller, where the feedback gains is:

$$K = -R^{-1} B^T P \tag{3.28}$$

where the Riccati matrix, P is the solution to the algebraic Riccati equation:

$$A^T P + PA - PBR^{-1} B^T P + Q = 0 \tag{3.29}$$

This matrix represents the optimal infinite horizon cost, $J = x_0^T P x_0$ to control the system from x_0 to the origin.

As the models in Section 3.1 are not linear, LQ control cannot directly be applied. Therefore, the matrices A and B are computed by linearizing the error models around an operating point. In the work, the error models are linearized around a straight reference path with a constant longitudinal velocity:

$$A = \left.\frac{\partial f_e(x,u)}{\partial x}\right|_{c=0,\, d=0,\, \psi_{1,e}=0,\, \Gamma_{1,e}=0,\, v_x=v_x} \tag{3.30a}$$

$$B = \left.\frac{\partial f_e(x,u)}{\partial u}\right|_{c=0,\, d=0,\, \psi_{1,e}=0,\, \Gamma_{1,e}=0,\, v_x=v_x} \tag{3.30b}$$

where $f_e(\cdot)$ is the nonlinear error model. As the longitudinal velocity has large effects on the vehicle, the controller would not perform well if it was linearized for only one velocity. To solve this issue, the LQ problem is solved for a large range of velocities. Gain scheduling techniques are then used to interpolate between the gains at the different operating points. The resulting gain scheduled controller will no longer minimize the cost in (3.27) and the performance is only guaranteed for the linearized operating points.

3.2.1 Feedforward

The feedforward term is formulated based on the model. This results in three different expressions, one for the kinematic models, one for the dynamic tractor, and one for the dynamic trailers, which can be found in [29]. For the kinematic models, the relation between steering angle and curvature in steady-state is formulated as:

$$u_0 = (a_{11} + a_{12})c(s) \tag{3.31}$$

For the dynamic models the understeer gradient, K_{us} is additionally incorporated, resulting in:

$$u_0 = (a_{11} + a_{12})c(s) + K_{us}v_x^2 c(s) \tag{3.32}$$

The understeer gradient describes the handling characteristics of the vehicle and is a function of the tractor weight distribution and the cornering stiffnesses of front and rear tires [29]:

$$K_{us} = \left(\frac{W_f}{C_{\alpha,f}g} - \frac{W_r}{C_{\alpha,r}g}\right) \tag{3.33}$$

where W_f and W_r are the vertical force on the front and rear axles, respectively. By including the understeer gradient, the feedforward is capable of compensating for the vehicle understeer or oversteer that occurs at higher speeds. The difference between the feedforward for the dynamic tractor and the dynamic trailer models is in how the vertical forces are calculated. For the tractor model, they are defined as follows:

$$W_f = m_1 g\frac{a_{12}}{a_{11}+a_{12}} \qquad W_r = m_1 g\frac{a_{12}}{a_{11}+a_{12}} \tag{3.34}$$

For the trailer model the trailer mass is included, which results in:

$$W_f = m_1 g\frac{a_{12}}{a_{11}+a_{12}} \qquad W_r = m_1 g\frac{a_{12}}{a_{11}+a_{12}} + m_2 g\frac{a_{21}}{b_2+a_{21}} \tag{3.35}$$

Curvature saturation

The feedforward term described above naively tries to follow the reference, regardless of how aggressive it is. When a trailer is added, this can lead to excessive oscillations of the trailer system. For this reason, the impact of the feedforward term on the total control law is adjusted depending on the current speed and curvature. This is done by limiting the value of the curvature with regards to a maximum allowed lateral acceleration before computing the feedforward value.

$$\bar{c}(s) = \begin{cases} c(s), & \text{if } -\frac{a_{y,max}}{v_x^2} \leqslant c(s) \leqslant \frac{a_{y,max}}{v_x^2} \\ \operatorname{sign} c(s) \cdot \frac{a_{y,max}}{v_x^2}, & \text{otherwise} \end{cases} \tag{3.36}$$

3.3 Model predictive control

Model predictive control is a general control methodology where an optimal control problem (OCP) is solved online with a system in a closed-loop. Traditionally MPC was used in the process industry to control slow systems. However, increased availability of powerful computing hardware and optimization solvers, have introduced MPC to many other applications. It is widely used for the control of vehicles and is considered an especially effective method when the vehicle model is more complex [4]. One additional benefit with MPC is the ability to have control and state constraints in the OCP. This can improve the controller's performance over other solutions, such as naive clamping of the control signal.

The nonlinear MPC problem is defined as follows:

$$\begin{aligned} \min_{u(t)} \quad & \phi(x(t_0+T), t_0+T) + \int_{t_0}^{t_0+T} L(x(t), u(t), t)dt \\ \text{s.t.} \quad & \dot{x}(t) = f(x(t), u(t), t), \\ & x(t) \in \mathbb{X}, \quad u(t) \in \mathbb{U}, \\ & x(t_0) = x_0 \end{aligned} \tag{3.37}$$

where ϕ is the terminal cost function, L the stage cost function and T the time horizon, $\mathbb{X}$ and $\mathbb{U}$ represent the constraints on the states and controls, respectively, and x_0 is the initial state. As opposed to the infinite horizon LQ problem in (3.27), the MPC problem has a finite horizon, T. This parameter balances how well the solution approximates an infinite horizon solution and the computational requirements of the controller. The problem is solved repeatedly at every time step, with x_0 set to the current state. Here, only $u(t_0)$ is applied to the system at every time step, while the rest is discarded.

To solve the problem in (3.38), it is first discretized with an Euler forward method and cast as a nonlinear program using direct multiple shooting [42]. The created nonlinear program can then be solved with a general nonlinear solver, such as IPOPT [43]. As with most nonlinear optimization problems there is no guarantee that the solver will converge to the global optimum, therefore it is important to initialize the problem with a good initial guess. When the problem is solved in an MPC, it can be warm-started with the solution from the previous time-step.

The implemented MPC controller uses constraints on both the steering angle, δ_f and rate, $\dot{\delta}_f$, while no constraints are used on the other vehicle states.

3.3.1 Linear MPC

As the nonlinear optimal control problem in (3.38) can be hard to solve, a simpler linear MPC problem is defined as:

$$\begin{aligned} \min_{u(t)} \quad & \|x(t_0+T)\|^2_{Q_T} + \int_{t_0}^{t_0+T} \|x(t)\|^2_Q + \|u(t)\|^2_R dt \\ \text{s.t.} \quad & \dot{x}(t) = A(t)x(t) + B(t)u(t), \\ & x(t) \in \mathbb{X}, \quad u(t) \in \mathbb{U}, \\ & x(t_0) = x_0 \end{aligned} \tag{3.38}$$

where Q_T is the terminal weight, Q the state weight, and R the control weight. Moreover, $A(t)$ and $B(t)$ define the linear state space model. Linear MPC requires that the problem in (3.38) fulfills three conditions:

- The cost functions are quadratic.
- The model is linear and may be time-variant.
- The sets of allowed controls and states are convex polytopes, i.e. the constraints are linear.

The resulting problem can be solved using quadratic programming. Quadratic programming gives the MPC many guarantees that do not exist for the nonlinear problem. Most importantly it guarantees convergence to the global optimum if it exists. Additionally, when quadratic programming is used, it is possible to calculate a worst-case bound on the number of iterations until convergence. This makes sure, that the MPC controller is safely implementable in a real-time system [44, 45].

When a linear MPC controller is created, the weight matrix for the terminal cost Q_T is set to the Riccati matrix, which is calculated by solving (3.29). This is done using the error model linearized around a straight reference path with the longitudinal velocity set to 70 km/h, in the same manner as in (3.30).

3.3.2 Reference signal

For the MPC controller, the future reference signal is included in the optimization problem to give the controller preview capability. The reference signal for the error model discussed in Section 3.1, consists of curvature, the derivative of curvature, and the hitch angle reference. It is created by assuming that the vehicle travels at the current speed along the reference line. The references are then extracted at the following arc lengths:

$$s = s_0 + v_x T_s k \qquad k \in 0, 1, \ldots, \frac{T}{T_s} \tag{3.39}$$

where s_0 is the current arc length and T_s is the sampling time of the controller.

4 Results

This chapter presents the results that are obtained by using the previously defined methods. The results are divided into two separate parts. In Section 4.1 the models are presented with their parameters together with their predictive performance. Then in Section 4.2, the performance of using these models with an LQ and MPC controller is presented and discussed.

4.1 Modeling

This section consists of a short description of the dataset, the implementation of the identification procedure from Section 2.2, how the models are validated, and the results from the validation together with a discussion of the results.

4.1.1 Dataset

A system identification dataset is created with TruckMaker. As the goal of the models is to describe the system well during aggressive maneuvering, the dataset should reflect this and excite the dynamics of the vehicle. Therefore, the dataset consists of double lane change maneuvers and driving with aggressive sinusoidal steering at speeds ranging from 40 km/h to 100 km/h for a total of 20 maneuvers. The dataset includes the states and control signals of the models with a sampling time of 10 ms.

The dataset is split into a separate training and validation set, and only the training data is used during identification, while the validation is used for the evaluation of the models.

As the kinematic models assume that no tire slip occurs, the aggressive high-speed maneuvers are excluded from the dataset when they are identified. This is done to ensure that these models are accurate for conservative driving, where kinematic models should behave well.

4.1.2 Implementation

The nonlinear optimization problem in (2.15) is constructed for the different models in CasADi [46] and solved using IPOPT [43]. A step size of 10 ms is selected for the one-step predictor to match the sampling time of the data. The same procedure is performed for all models with one exception, the dynamic roll model. The reason for this is that the optimizer has trouble finding a good minimum for the roll model,

when all parameters are free. Because of this, the parameters of this model are identified in a two-stage approach. First, the parameters shared with the dynamic trailer model are identified by using the dynamic trailer model and disregarding roll. Then, these parameters are fixed while the rest of the parameters are identified. This is similar to the estimation approach in [33], where the same two-stage method is used but for slightly different parameters. A third stage where all parameters are free and initialized with the solution from the second stage could be added. However, this barely improved the model fit and is therefore disregarded.

4.1.3 Validation

Validation is done by evaluating the prediction performance of the model in a longer time horizon than the 10 ms horizon they are identified with. It is important that the models perform well during longer horizons, as they are used to simulate the system forwards in the MPC controller. A prediction horizon of 1 s is selected as a reasonable length.

The evaluation is performed on double lane change maneuvers of varying speeds. The performance of the predictions at varying parts of the maneuvers are averaged using a root-mean-square error (RMSE).

4.1.4 Model performance

The system identification procedure is performed for all models. An overview of the performance of the models can be seen in Table 4.1, which presents the prediction errors of the models for all test data. It can be seen that the prediction errors of the kinematic models are particularly high, especially for the position of the tractor. This is quite natural as the full dataset includes high-speed aggressive driving with large sideslip angles, which severely violates the no-slip assumptions in the kinematic models. Between the dynamic models, the performance of predicting tractor pose differs much less. The largest difference is found when a trailer is included in the model, which in addition to modeling the hitch dynamics, also reduces the prediction error in position by around a third. Furthermore, the dynamic trailer model with a nonlinear tire model improves the performance slightly over the same model with a linear tire model. Finally, the trailer model with roll has practically the same performance as the one without. One possibility for this is that there is too little energy in the rolling motion relative to the rest of the system. This can be seen by comparing the energy in rotation along the roll axis with rotation around the hitch point for the trailer. This is done in Figure 4.1, where it can be seen that the kinetic energy in the roll motion is almost negligible in comparison to motion around the hitch point. This explains one possible reason why adding dynamic hitch states to the model improves the prediction performance, while adding roll leaves it largely unchanged.

Comparison of dynamic and kinematic model

The errors in the previous table only describe how the models performed on the whole dataset. To get a more detailed understanding of how the models behave, the prediction errors are plotted against the speed of the maneuvers. In Figure 4.2, the

Table 4.1: RMSE of 1 s predictions using the different models.

Model	Position (m)	Heading angle (°)	Hitch angle (°)	Tractor roll angle (°)	Trailer roll angle (°)
Kinematic tractor	0.306	0.75	—	—	—
Dynamic tractor	0.060	0.31	—	—	—
Kinematic trailer	0.306	0.75	0.96	—	—
Dynamic trailer	0.039	0.27	0.50	—	—
Dynamic trailer w/nl tire	0.037	0.26	0.44	—	—
Dynamic trailer w/roll	0.038	0.27	0.49	0.28	0.94

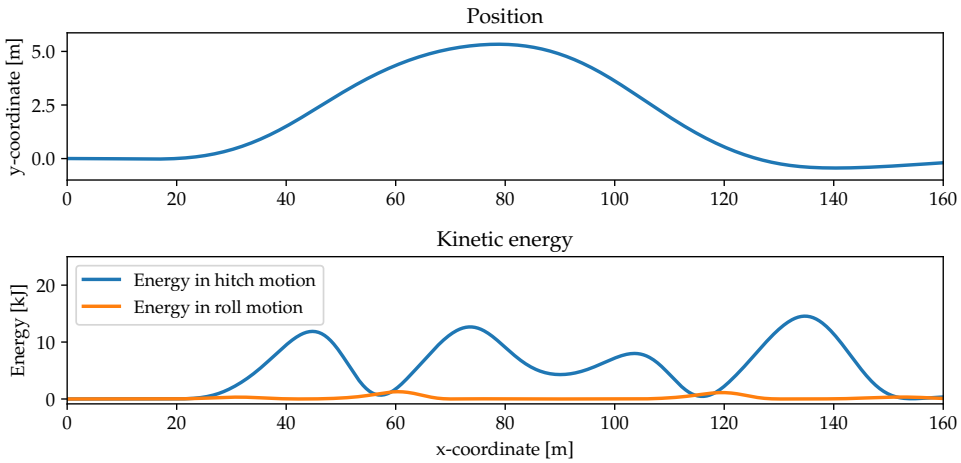

Figure 4.1: The energy in roll motion and rotation around the hitch point for a trailer during a double lane change maneuver in 70 km/h.

kinematic tractor and tractor-trailer models are compared with their dynamic counterparts. This shows that the kinematic models have around the same prediction error in position and heading as the dynamic models until around 55 km/h. After this point, the kinematic models' performance quickly worsens relative to the dynamic models. Some increase in prediction error of position is expected as the speed increases, because the vehicle travels a longer distance during the 1 s horizon. However, this cannot explain the decrease in relative performance.

A similar behavior can be seen in the prediction error of the hitch angle, but it is slightly different with the kinematic model performing better at low speeds, and it does not perform worse until 75 km/h. The lower prediction error at low speeds could be explained by the fact that the kinematic model is only fit to data with low speed maneuvers, while the dynamic model is fit to a larger range of data. This is indicative of the fact that the dynamic trailer model lacks the expressive power to accurately describe the full dataset. The cause of this is likely that the nonlinear behavior of the tires is prominent during more aggressive driving, which is further discussed in the next section. Additionally, the assumption of small hitch angles, and that the longitudinal velocities of the tractor and trailer are the same, may contribute to this issue.

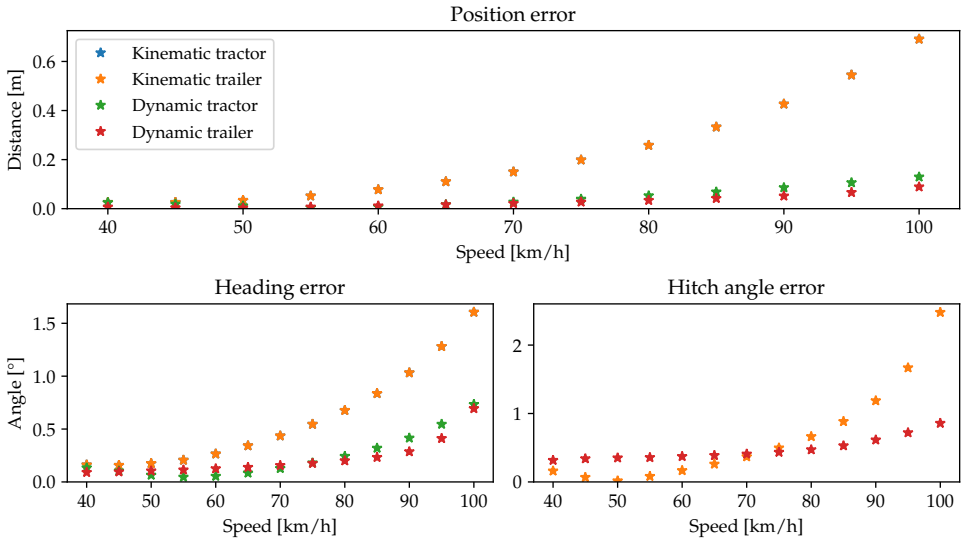

Figure 4.2: The RMSE of 1 s predictions plotted against longitudinal speed for the kinematic models, dynamic tractor model, and dynamic trailer model. Note that both kinematic models have the exact same errors in position and heading.

The difference between the kinematic and dynamic models is further illustrated in Figure 4.3. In this figure, 1 s predictions of position for both types of models are plotted against the true values for a low (40 km/h) and high (70 km/h) speed. For the low speed the models behave the same and there is barely any deviation from the reference values. However, for the higher speed the kinematic model starts to predict that the vehicle will turn more than the reference. At the same time, the dynamic model appears to track the reference very well. This is the general behavior of the kinematic models during more aggressive driving as they ignore sideslip and the tendency of many vehicles to understeer [29].

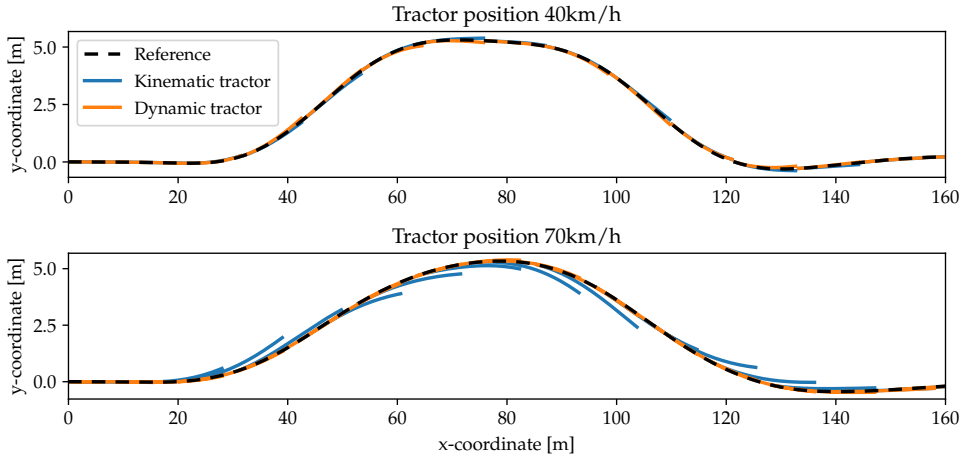

Figure 4.3: 1 s predictions of the tractor position for a low and high speed maneuver, using a kinematic and dynamic model.

Comparison of dynamic models

The performance of the different dynamic models is presented in Figures 4.4 and 4.5. The first of these shows a general comparison of the models, and the latter, the roll angle predictive performance. Overall, this shows a similar result as is presented in Table 4.1, with the trailer models having a smaller prediction error than the tractor model, while at the same time not differing much from each other. The tractor model has about the same performance in position error and slightly better in heading error for speeds around 50 km/h to 70 km/h. Outside of this region the predictive ability of this model worsens. However, it is still decent, reaching an average position error of 0.11 m for 1 s predictions at 100 km/h. As an illustration, the vehicle travels ∼28 m during the prediction horizon.

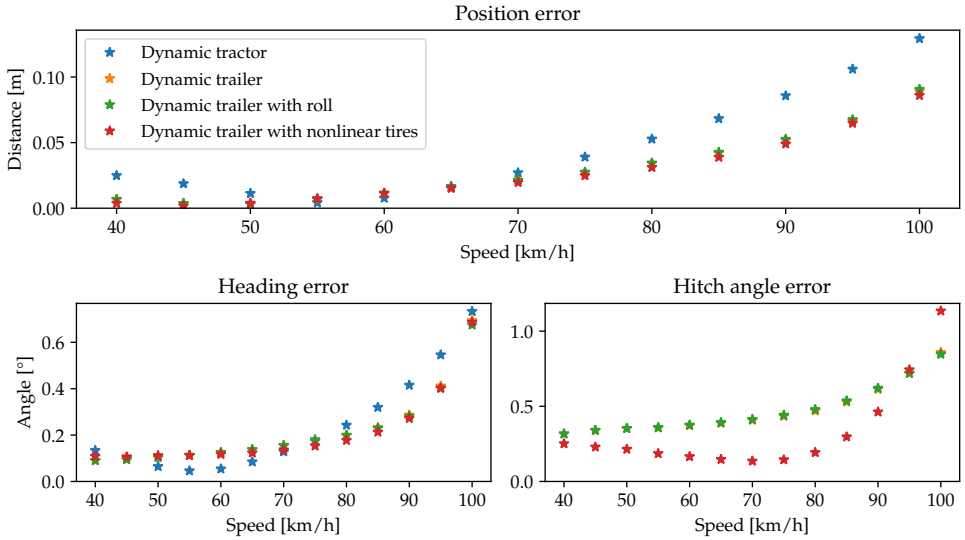

Figure 4.4: The RMSE of 1 s predictions for the different dynamic models and for different speeds. Note that the dynamic trailer model with roll overlaps the dynamic model.

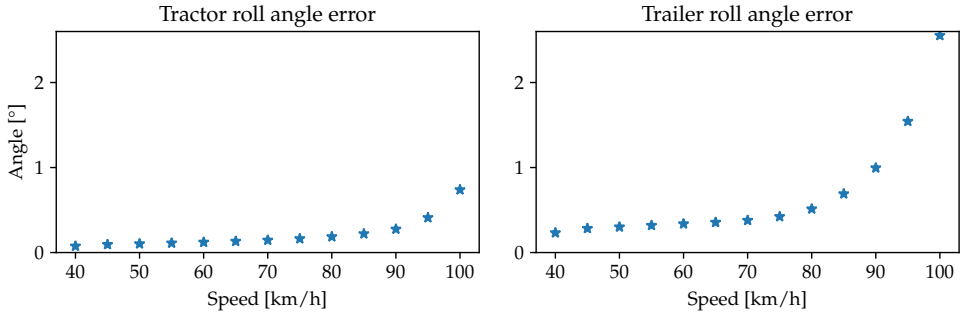

Figure 4.5: The RMSE 1 s prediction error of the tractor and trailer roll angle for different speeds.

Just as the results in Section 4.1.4, the largest difference for the trailer models is between the one with a nonlinear tire model and the rest. For these, the difference in position and heading error are consistently quite small, but the linear model performs

slightly worse at almost every speed. For the hitch angle prediction, the difference is larger and the linear model performs much worse at most speeds, while having a slightly better performance at 100 km/h. This is most likely related to the worse predictive performance of the dynamic trailer model compared with the kinematic model at low speeds, discussed in the previous section. The cause of this is likely that the full dataset includes aggressive driving, where the nonlinear properties of the tires are substantial. The nonlinear effects are probably larger for the trailer as the higher speeds cause it to oscillate heavily. When a linear tire model is fit to this data it distorts the model and worsens model fit for low slip angles. This is visualized in Figure 4.6, which shows a distorted linear tire model with a nonlinear true model. It is also reflected in the cornering stiffnesses that are identified for the linear and nonlinear models. When a nonlinear tire model is used, the cornering stiffnesses increase by 2.6 %, 12.6 %, and 38.3 % for the front, rear, and trailer wheels, respectively. This is another indication that nonlinear effects are more prominent for the trailer

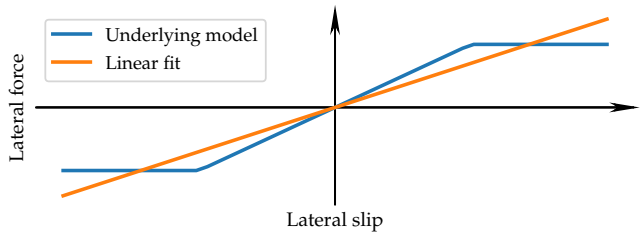

Figure 4.6: The effect of fitting a linear tire model to a nonlinear underlying model.

As the system is evaluated in simulation, the tire slips can be plotted to show the actual behavior. A plot of this can be seen in Figure 4.7, which shows the tire slips of the front wheels, the rearmost tractor wheels, and the rearmost trailer wheels, for a double lane change in 100 km/h. The previous result is reflected in this figure, with the trailer tires having larger slip angles than the tractor tires.

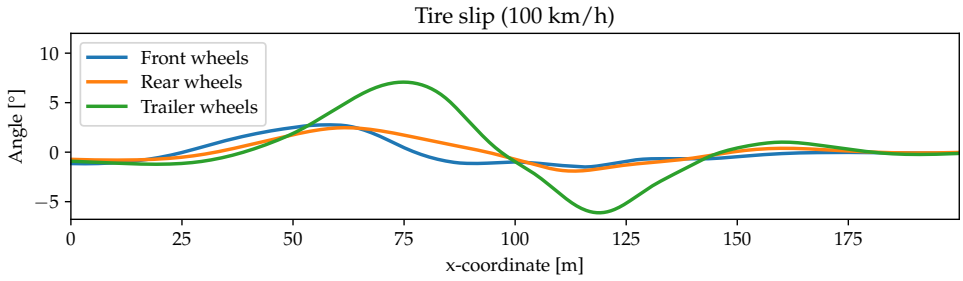

Figure 4.7: The tire slip angles for a double lane change in 100 km/h.

For the roll model, prediction performance of the position, heading, and hitch angle hardly changes in comparison to the dynamic trailer model, just as in Section 4.1.4. The predictive performance of roll, shown in Figure 4.5, is good for low speeds, but worsens as speed increases. It is also better at predicting the tractor roll angle than the trailer roll angle. To get some perspective, the largest expected roll angle of the tractor and trailer are around 10°, when the suspension nears its end-stop. Some increase in prediction error over velocity is anticipated as the magnitude of roll angles

increases with more aggressive driving. However, after 85 km/h the errors of both the tractor and trailer roll angles increase much faster than before. This suggests that the nonlinear effects, discussed in Section 2.1.5 start to have a larger effect, mostly due to the suspension approaching its end-stop.

4.2 Control

General controller performance is presented in Section 4.2.3 for a range of maneuvers at various speeds using the different models. Furthermore, an extended discussion follows in Section 4.2.3, regarding how varying the parameters in the MPC controller affects its performance. Finally, in Section 4.2.4 robustness evaluation is presented.

4.2.1 Implementation

The LQ controller described in Section 3.2 is implemented for the different models. The controller weights for the different controllers are presented in Table 4.2, which represent the respective diagonal element in the $\overline{Q}$ matrix. It was implemented with a running rate of 100 Hz. Additionally, the steering signal and rate were constrained to $\pm 45°$ and $\pm 45\,°/s$, respectively, which are defined in Equation (2.10). This was done by clipping the steering signal, u_k and the rate, $\frac{u_k - u_{k-1}}{T_s}$.

Table 4.2: The controller weights for the LQ controller, with $R = 1$

Model	d	$\dot{d}$	d_t	$\psi_{1,e}$	$\dot{\psi}_{1,e}$	Γ_e	$\dot{\Gamma}_e$	$\phi_{1,e}$	$\dot{\phi}_{1,e}$	$\phi_{2,e}$	$\dot{\phi}_{2,e}$
Kinematic tractor	0.02	–	–	0.3	–	–	–	–	–	–	–
Kinematic trailer	0.02	–	0	0.3	–	0.1	–	–	–	–	–
Dynamic tractor	0.02	0.3	–	0.3	1.5	–	–	–	–	–	–
Dynamic trailer	0.02	0.3	0	0.3	1.5	0	2	–	–	–	–
Dynamic trailer w/d_t	0.02	0.1	0.25	0.1	0.5	0	1.5	–	–	–	–
Dynamic trailer w/roll	0.02	0.3	0	0.3	1.5	0	2	0	0	0	2

The MPC problem in (3.38) is constructed for the different models in CasADi [46]. A time horizon of 5 s is selected, to give the controller a long preview of the maneuver. The error models from Section 3.1 are used and discretized using an Euler forward method with a sampling time of 100 ms. An extra state representing the steering signal is added to the model and the steering angle rate is used as the input to the model. Additionally, constraints are added to the steering angle and rate with the same limits as above. The controller weights for the different MPC controllers are presented in Table 4.3, which represent the respective diagonal element in the $\overline{Q}$ matrix. All general performance and robustness evaluation is done using the models with no weight on d_t. The dynamic trailer model with the d_t tuning is compared with the regular tuning in Section 4.2.3.

When a linear tire model is used, the error model is linearized around the reference. The resulting quadratic optimization problem is then solved using qrqp, a QP solver bundled with CasADi. For the model with a nonlinear tire model, the errors and steering angle are assumed to be small, and small angle approximations are performed to simplify the trigonometric expressions. The nonlinearity from the tire

Table 4.3: The controller weights for the MPC controller, with $R = 1$

Model	d	$\dot{d}$	d_t	$\psi_{1,e}$	$\dot{\psi}_{1,e}$	Γ_e	$\dot{\Gamma}_e$	$\phi_{1,e}$	$\dot{\phi}_{1,e}$	$\phi_{2,e}$	$\dot{\phi}_{2,e}$	δ_f
Kinematic tractor	0.2	–	–	0.1	–	–	–	–	–	–	–	0.5
Kinematic trailer	0.2	–	0	0.1	–	10	–	–	–	–	–	0.5
Dynamic tractor	0.3	0	–	0	0.1	–	–	–	–	–	–	1
Dynamic trailer	0.3	0	0	0	0.1	1	0.25	–	–	–	–	1
Dynamic trailer conservative	0.3	0	0	0	0.1	1	6	–	–	–	–	1
Dynamic trailer w/nl tire	0.3	0	0	0	0.1	1	4	–	–	–	–	1
Dynamic trailer w/d_t	1	0	0.3	0	0.1	0	0	–	–	–	–	1
Dynamic trailer w/roll	0.3	0	0	0	0.1	1	0.25	0	0	0	0.5	1

model is still included in the problem. The resulting nonlinear optimization problem is solved with IPOPT [43]. Finally, the running rate of the MPC controller was set to 10 Hz.

4.2.2 Evaluation

The controllers are evaluated by investigating their performance in the simulation environment. The tests are performed for different maneuvers using a constant longitudinal velocity in the range of 50 km/h to 100 km/h with a resolution of 5 km/h. The performance is evaluated according to several criteria. First, a run is considered a failure if the vehicle rolls over. If rollover is avoided, then the performance is assessed with the following measures: tractor cross-track error, trailer cross-track error, and maximum roll angle of the trailer. The tractor and trailer cross-track errors indicate how well the vehicle follows the path. For a run they are averaged using root-mean-square. The maximum roll angle is used as a measure of vehicle stability. The reason that the trailer roll angle is used is because rollover of a tractor-trailer tends to start at the rear of the trailer [21]. Roll angles at 10° and above are considered critical as this is when the trailer nears rollover.

Maneuver description

Three different paths representing double-lane change maneuvers of varying aggressiveness are created for evaluation. The rollover threshold index is used as a measure to determine path aggressiveness. This index describes the lowest value of lateral acceleration which causes the vehicle to rollover for steady-state cornering. A typical U.S. style five-axle tractor-trailer combination has a rollover threshold in the range of 0.25 g to 0.5 g [32]. To determine the configuration of the double lane change, the maximum lateral acceleration is calculated by using the maximum speed of 100 km/h together with the largest curvature of the path ($a_y = cv^2$). The width of the maneuver is selected to be 3 m, which roughly corresponds to the width of a normal drive lane. The length is then selected such that the maximum lateral acceleration would be $4\,\mathrm{m/s^2}$ which is the approximate rollover threshold of the investigated vehicle. After this, two more maneuvers are created by adjusting the length to create one more and one less aggressive maneuver. The three different maneuvers are shown in Figure 4.8, with the maximum curvature and lateral acceleration shown in Table 4.4.

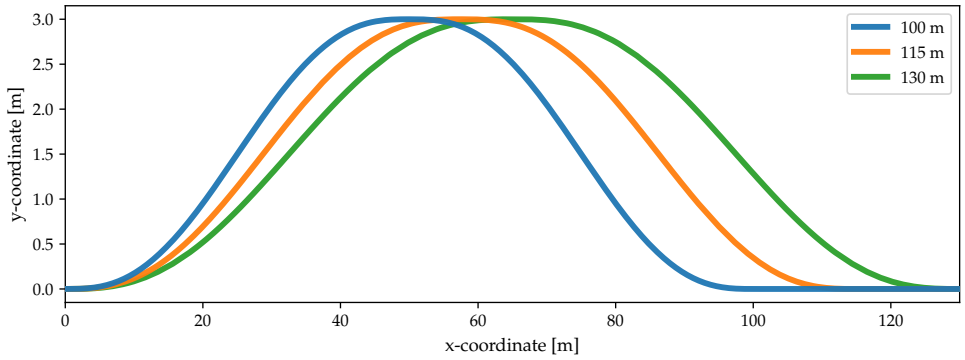

Figure 4.8: The three different double lane changes that the controllers are evaluated on.

Table 4.4: The length, curvature and maximum lateral acceleration of the three maneuvers.

Maneuver length (m)	Max curvature (1/m)	Max lateral acceleration (m/s^2)
100	0.0069	5.32
115	0.0052	4.01
130	0.0041	3.16

4.2.3 General performance

The following section is dedicated to results and discussion of the LQ and MPC controllers' performance for the maneuvers specified in Section 4.2.2.

LQR performance

In Figure 4.9 the performance of the LQ controller is presented for different speeds during a double lane change of 100 m. As the speed increases, the cross-track errors and roll angles increase for all the models. However, the performance and general behavior differs between the models.

The controllers that use kinematic models perform well for lower speeds up to 55 km/h. After that, the tractor error quickly increases at a much higher rate than the other models. This is likely related to the fact that the predictive performance of position and heading for the kinematic models also worsen at around 55 km/h, as discussed in Section 4.1.4. Both the controllers with kinematic models fail for speeds above 90 km/h, as the controllers cannot handle the increased trailer momentum, which results in the vehicle rolling over.

For the controller using a dynamic tractor model, the tractor cross-track error is kept consistently low for all speeds. This leads to a more aggressive behavior, which can be seen from the large roll angles for speeds above 85 km/h. This behavior becomes unmanageable for ~95 km/h as the vehicle nears rollover.

The controllers using dynamic trailer models have the smallest trailer errors and trailer roll angles compared to the others. This improved performance however, comes at a cost of a larger tractor error. The controllers have the same general per-

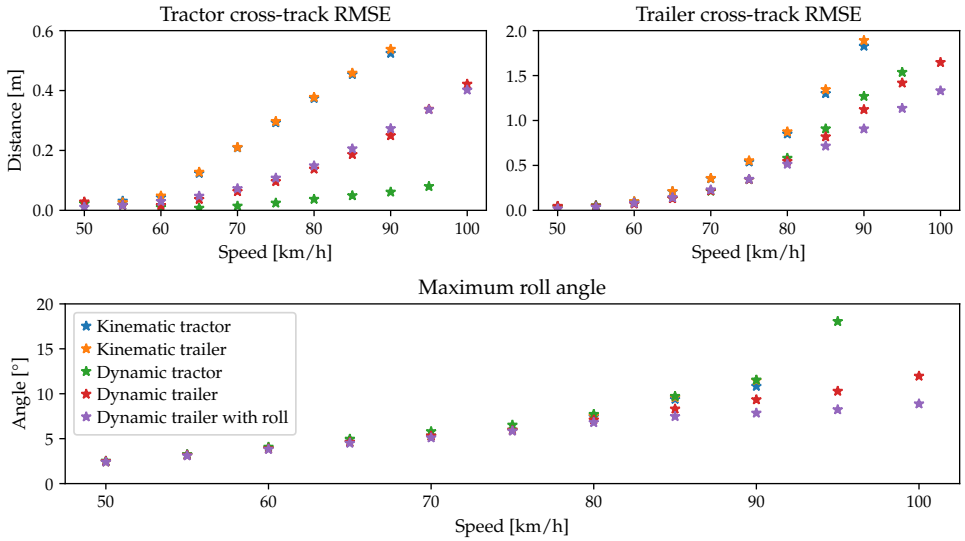

Figure 4.9: The performance of the LQ controllers at different speeds, for the 100 m long maneuver.

formance for all speeds up to 85 km/h where they start to differ. At this speed, the controller using the dynamic trailer model including roll outperform all other models in terms of trailer error and roll angle.

Despite model choice, it is noted that the LQ controller had difficulties in minimizing the effects of trailer oscillations during faster maneuvers. This is one of the main reasons behind the large trailer errors and trailer roll angles. The controllers that use the dynamic trailer models are better in this regard, however, the decrease in trailer error barely compensates for the increase in tractor error. Instead, the additional states allow the controller to behave more conservatively. In turn, this allows the controller to complete the maneuver at higher speeds without rolling over. This is also the effect of including the roll angles, as it is another state that forces the system to be more conservative.

The underlying issue with the LQ controller is that it tries to minimize the current errors, without regard to the future reference. This is problematic, since the controller will still follow the path, even when it is close to becoming infeasible.

Trailer cross-track error tuning In Section 3.1.6 a procedure is presented for direct weighting of the trailer cross-track error. This is implemented for the LQ controller and the method is further referenced to as d_t-tuning. This controller is then tested by using the dynamic trailer model for the 100 m double lane change. Furthermore, performance is compared to the regularly tuned controlled, and the result is presented in Figure 4.10.

The performance of the two tuning strategies are comparable over all measures, although the d_t-tuned controller shows a minor performance increase. The improved performance of the d_t-tuned controller becomes prominent for higher speeds. Although the errors are quite large overall, it does manage to decrease all errors and the roll angle for 80 km/h and upwards.

Overall, the d_t-tuning has a decent positive effect on performance at higher speeds and generally improves the controller's response to tuning.

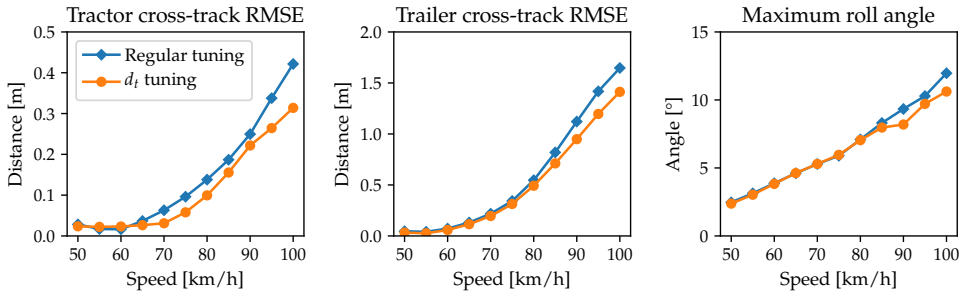

Figure 4.10: Comparison of the d_t-tuning and the regular tuning for the LQR controller with a dynamic trailer model.

MPC performance

In Figure 4.11, the performance of the MPC controller on the 100 m double lane change is presented. The overall performance when using the MPC controller differs greatly between the models.

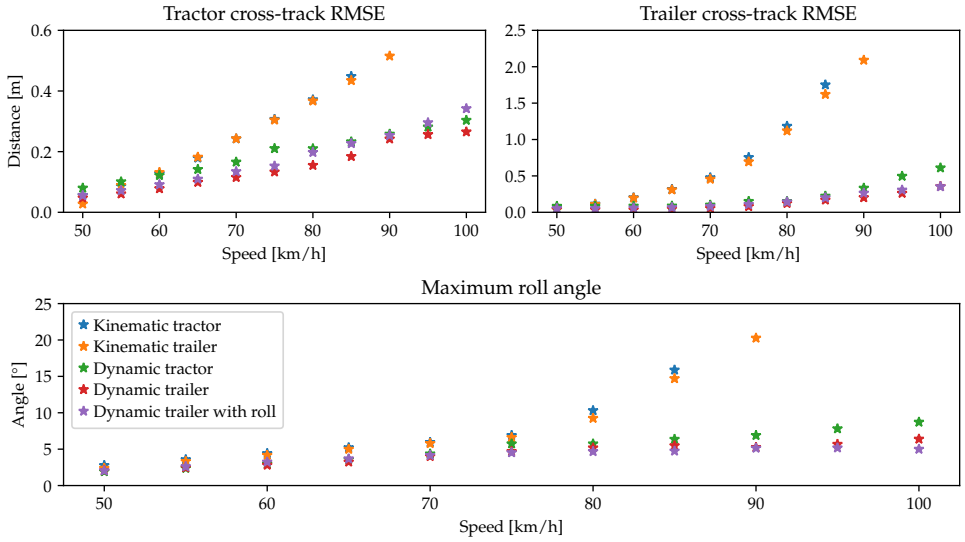

Figure 4.11: The performance of the MPC controllers at different speeds, for the 100 m long maneuver.

Just as with the LQ controller the kinematic models perform well for low speeds, but as the speed increases, the errors also steadily increase. These controllers start to deviate from the others around 60 km/h, and most notably struggles with large trailer errors. The maximum trailer roll angles for these controllers nears critical values at 80 km/h, and at ~90 km/h this leads to vehicle rollover.

The controller using the dynamic tractor model has seemingly good performance despite its lack of trailer information. What is interesting however, is that the trailer error does not become worse relative the trailer models, until at 90 km/h. Although

the controller has fair performance in many regards, it differentiates from the controllers using dynamic trailer models, by having large roll angles for the higher speeds. Most noteworthy, the controller that uses a dynamic tractor model has almost twice the roll angle ($\sim$10°) than the controller with the lowest value ($\sim$5°) for 100 km/h. This is discouraging, since a trailer roll angle of 10°, especially at such a high speed is considered critical in these tests.

For the controllers using dynamic trailer models, performance is comparable when considering trailer cross-track error. The controller using the roll model however, shows slight improvement in decreasing the roll angle at the highest speed. Interestingly, the controller using the dynamic trailer model (without roll) shows a better performance in reducing the tractor error, and performs best in this regard among all controllers.

Conclusively, the MPC controller performs better if the predictive performance of the used model is good. This is motivated by the considerable difference in performance when comparing controllers using dynamic models, with controllers using kinematic models. Additionally, the MPC controller shows a significant performance increase when equipped with a dynamic model that includes the trailer. Especially considering how it not only outperforms its tractor counterpart in decreasing the trailer error, but more significantly, the tractor error as well. Finally, although the performance increases when a trailer is included in the model, there is no substantial performance increase when extending the model to include roll. Despite the lack of an overall performance increase, the added roll states allow the controller to reduce the roll angles of the trailer. This is likely related to the discussion in Section 4.1.4, and the comparison made between the energies in rotation around the hitch point and trailer roll motion (see Figure 4.1).

Nonlinear model In Figure 4.12, the performance of the MPC controller using linear and nonlinear tire models are compared. This is done by using the dynamic trailer model on the 100 m maneuver. Overall, the performance is similar, with almost the same tractor error and maximum roll angle across all speeds. One slight difference appears for the trailer errors at larger speeds, where the error for the nonlinear model becomes approximately 10 cm larger than for the linear model. This may seem counterintuitive to the better predictive ability of the nonlinear model compared with the linear model presented in Section 4.1.4. Nevertheless, there are several explanations for this. First, as the linear dynamic trailer model is also used in the LQ controller, more time is spent tuning controllers with this model. In turn, this likely led to the linear model being slightly better tuned. Second, the increase in trailer error is probably caused by the larger cornering stiffnesses of the nonlinear model. These help the nonlinear model describes the trailer motion more accurately, compared to the linear model that will overestimate the trailer motion. However, this overestimation will make the controller more conservative, as it believes that the trailer will oscillate more than it does. Finally, as the MPC controller is run in a closed loop with the system, the feedback mechanism from this can compensate for the mismatch between the model and the system. This makes model improvements past a certain point have diminishing returns, as the controller is robust against small modeling errors.

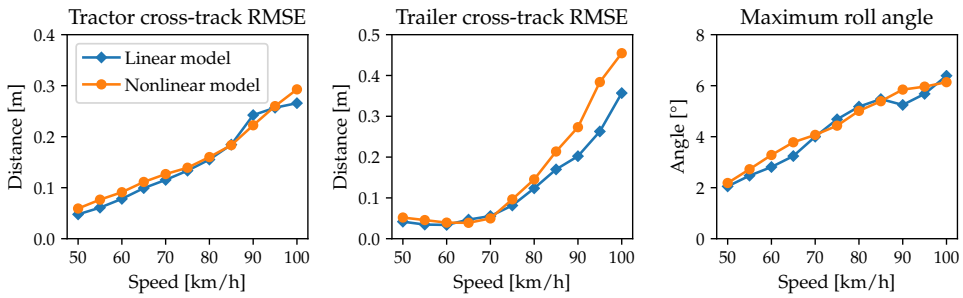

Figure 4.12: Comparison of using a linear and nonlinear tire model in the MPC controller with a dynamic trailer model.

Trailer cross-track error tuning Similarly to the LQ controller, a d_t-tuned MPC controller is implemented. This is done with the dynamic trailer model, and the controller is tested for the 100 m double lane change. A comparison of the performance between the regularly tuned, and d_t-tuned controller is presented in Figure 4.13. It can be seen that the performance is quite similar. The main difference is that trailer error is smaller at higher speeds for the d_t-tuning, at the expense of a slightly larger tractor error. To see how the tuning affects the behavior of the vehicle, the paths are compared for increasing velocities, which can be seen in Figure 4.14. In this plot, it can be seen that the d_t-tuning changes the behavior in two main ways. First, it reduces the large overshoot of the trailer at the end of the maneuver. Second, it centers the trailer trajectory slightly better on the reference path.

Conclusively, d_t-tuning for the MPC controller shows an increase in general performance at higher speeds. The greatest benefit however, is that tuning the trailer cross-track error is more intuitive since the performance variables are directly weighted.

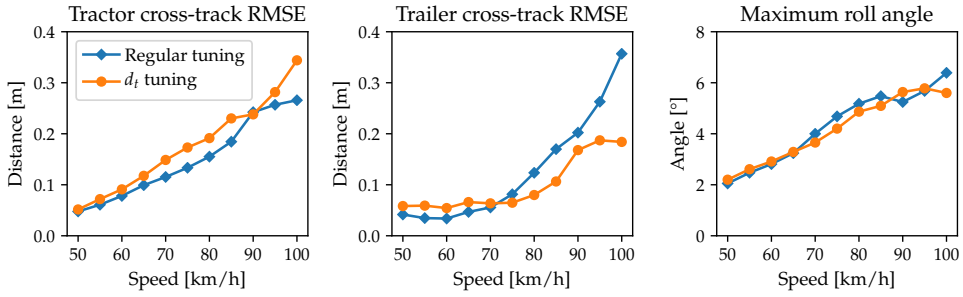

Figure 4.13: Comparison of the d_t-tuning and the regular tuning for the MPC controller with a dynamic trailer model.

Comparison of controller performance

By comparing the results presented in the previous section, the MPC controller on average outperforms the LQ controller on all measures. The difference in performance is highly related to the behaviors of the respective controllers. This can be visualized by comparing the trajectory of the tractor and trailer for the different controllers. This is done in Figure 4.15, using the dynamic trailer model for the 100 m maneuver

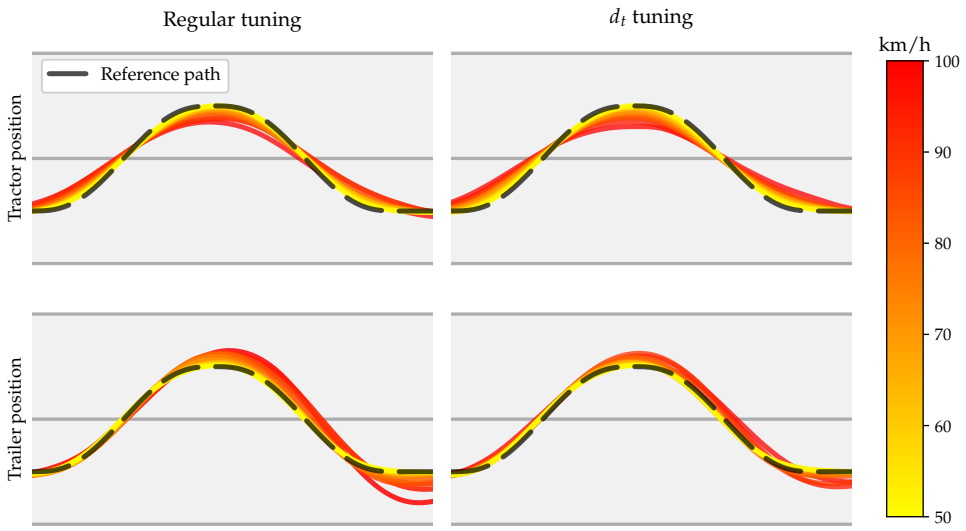

Figure 4.14: Comparison of the tractor and trailer paths for the two different tuning strategies.

at increasing speeds. This shows that for low speeds, both the LQ and MPC controllers track the reference well. However, when the speed increases their behaviors diverge. As the MPC controller is aware of the future path, it can realize that naively following the path will lead to massive trailer errors. Because of this, it can avoid this scenario by cutting through the curve. As the speed increases, it takes increasingly conservative actions.

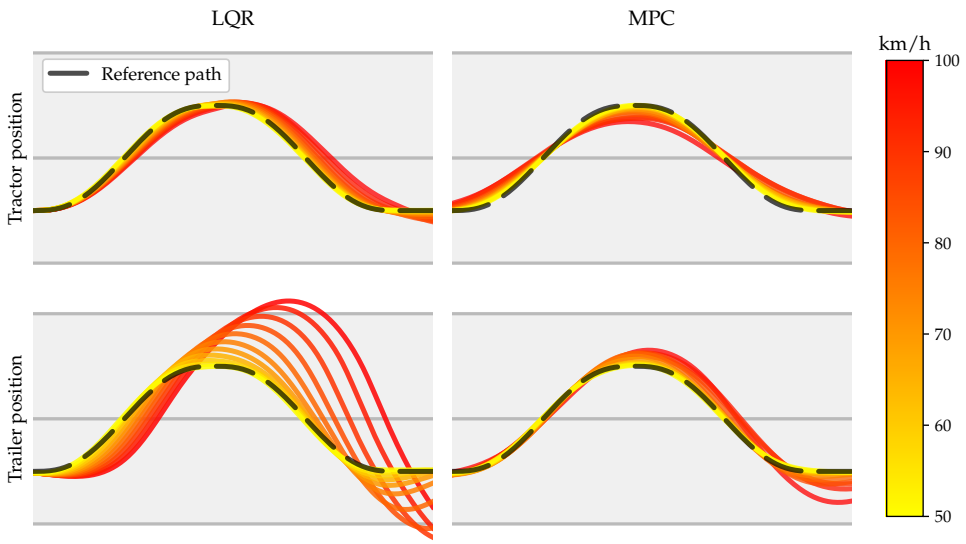

Figure 4.15: Comparison of the tractor and trailer paths for double lane changes of increasing speed, using a LQ and MPC controller with the dynamic trailer model.

The LQ controller, on the other hand, handles the situation completely differently. For higher speeds it starts to deviate from the path, just like the MPC. However, it does this in a much worse way. Instead of conservatively turning before the left

curve, it does it after. This becomes a large problem when the path suddenly changes direction from left to right, leading to a large heading error. When the controller tries to compensate for this heading error, it results in a large trailer swing. This is especially an issue because of the aggressiveness of the feedforward. A similar problem is found in [17], where it is shown that LQ with feedforward control has a tendency to overshoot the trajectory during aggressive maneuvers.

This shows one of the main differences between the LQ and MPC controllers. As the MPC is aware of the future reference, it can handle a path that is close to infeasibility, while the LQ is incapable of this.

Performance for additional maneuvers

The controllers are further tested on all maneuvers specified in Section 4.2.2 to investigate possible correlation between performance and path properties. Figures 4.16 and 4.17 show the performance of the LQ and MPC controllers for all maneuvers plotted against maximum lateral acceleration of the path. There is a notable dispersion of the data points in the cross-track errors plots. Although there is a clear a correlation between these errors and the acceleration, the variance is quite large. This implies that maximum lateral acceleration of the reference cannot by itself describe the cross-track errors.

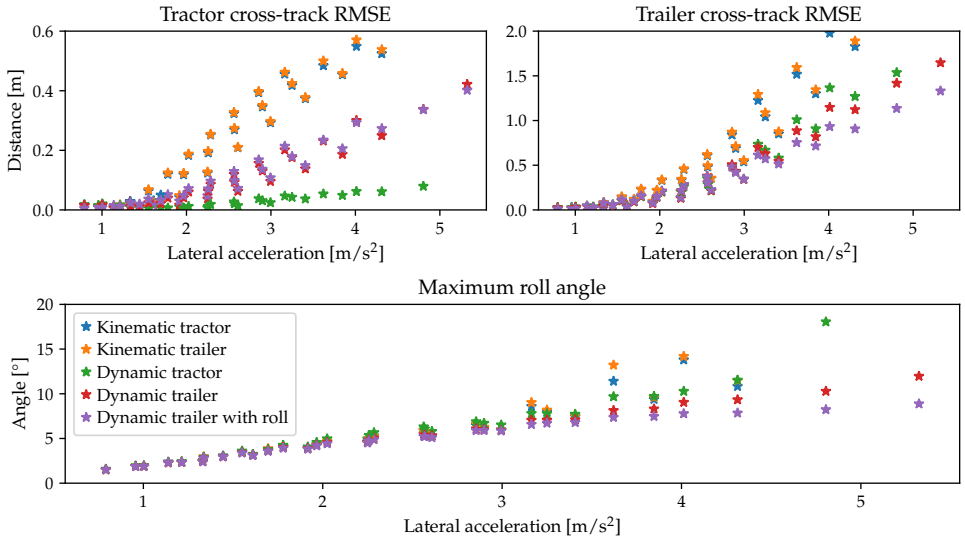

Figure 4.16: The performance of the LQ controllers plotted against the theoretical maximum lateral acceleration of the reference.

There seem to be a strong linear correlation between the maximum trailer roll angle and lateral acceleration. The relation is quite reasonable as the steady state roll angle is a linear function of the lateral force, which can be seen in Equation (2.6), when all rates are set to zero.

Interestingly, there seems to be much less variation when the errors are plotted against the lateral acceleration of the reference multiplied by the vehicle speed, i.e. $a_{y,max}v_x$. This can be seen in Figures 4.18 and 4.19. This interaction effect describes

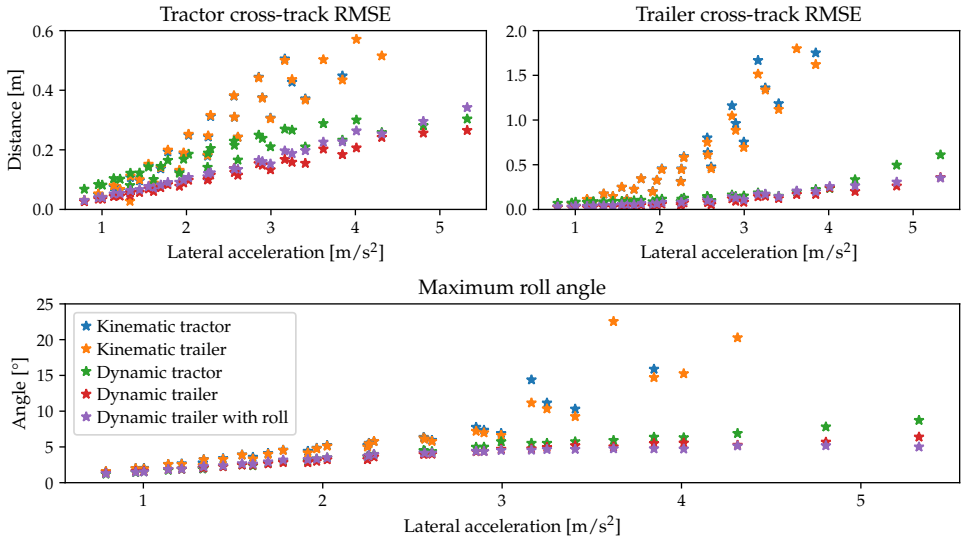

Figure 4.17: The performance of the MPC controllers plotted against the theoretical maximum lateral acceleration of the reference.

the cross-track errors particularly well, but show no additional improvement in describing the roll angle.

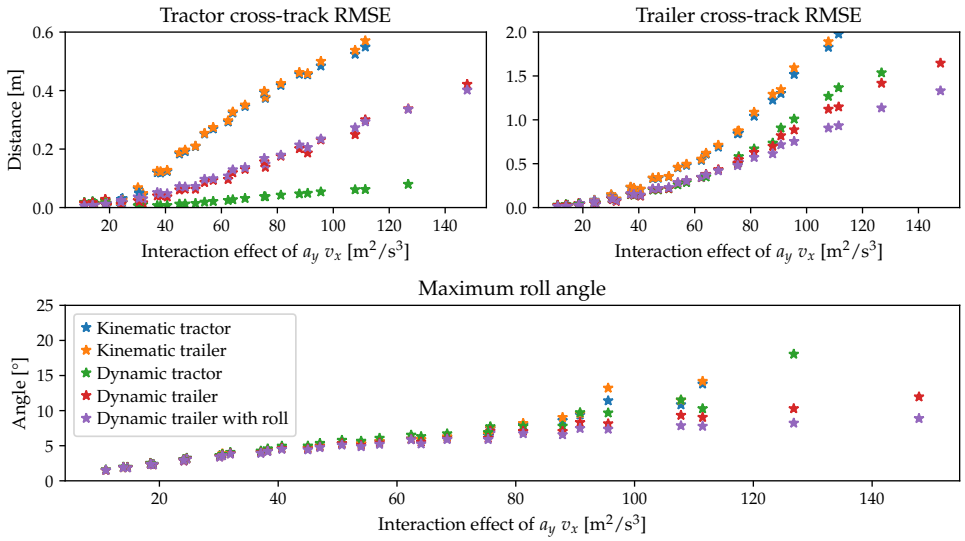

Figure 4.18: The performance of the LQR controllers plotted against an interaction effect of the velocity and the theoretical maximum lateral acceleration of the reference.

The requirement of velocity in addition to lateral acceleration to accurately predict the increasing controller errors, makes intuitive sense. The errors during more aggressive driving are largely caused by increased oscillation of the trailer. The energy in this oscillatory motion must come from the rest of the system. As the energy in the system is speed dependent, it is likely that the oscillations are also dependent on the speed, in addition to the lateral acceleration. A similar effect is seen for yaw instability of trailers, which can only happen at higher speeds [29].

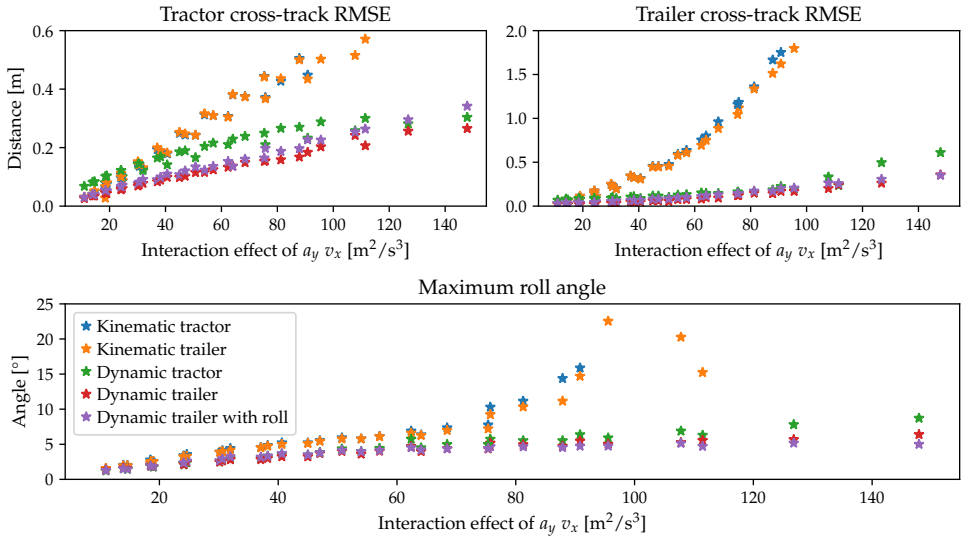

Figure 4.19: The performance of the MPC controllers plotted against an interaction effect of the velocity and the theoretical maximum lateral acceleration of the reference.

Parameters of the MPC controller

In Figure 4.20 the effect of changing the running rate, sampling rate, and time horizon on the performance of the MPC is presented. This is done using the dynamic trailer model for the 100 m maneuver with a speed of 85 km/h. When one parameter is varied, the others are kept constant at their respective nominal value.

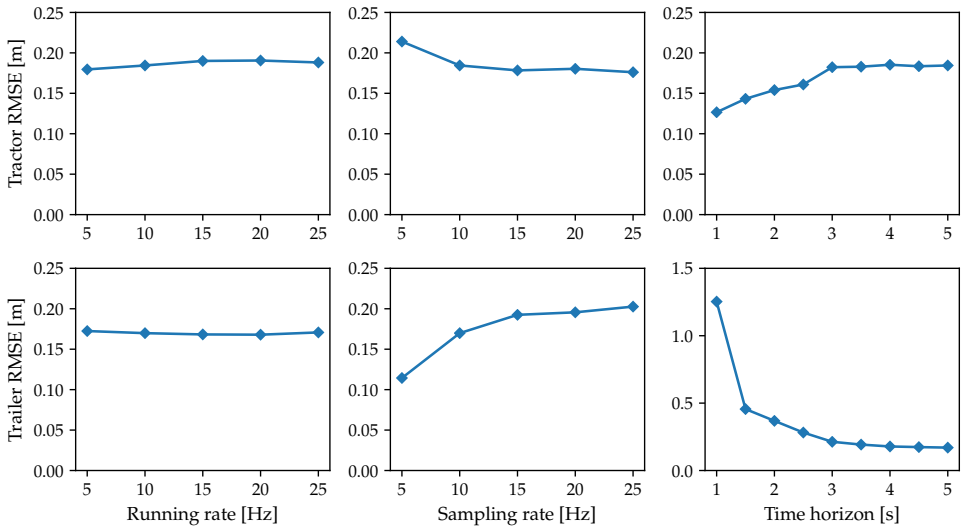

Figure 4.20: The effect of varying the MPC parameters on its performance. For a run at 85 km/h on the 100 m maneuver.

Running rate The performance is largely unaffected by the running rates of the controller in the tested interval. One reason is probably because the MPC controller outputs the steering rate instead of angle, which allows it to affect the future steering angle without running faster. However, this result might not transfer very well outside of this exact scenario as there are no measurement errors nor external disturbances in the simulation. When larger disturbances are present, the system might drift far off the predicted path if the running rate is too low, i.e. there is less feedback to compensate for model errors.

Sampling rate The performance is much more affected by the sampling rate. For large rates it is still mostly constant, although when the rate is decreased below 10 Hz, then the trailer error decreases slightly, at the cost of a larger tractor error. One possible reason for this could be that the larger discretization error from sampling slower, makes the model overestimate the trailer oscillation. This makes the controller more conservative, which increases the tractor error and decreases the trailer error. This is similar to [18], where it is found that a lower sampling rate could increase the performance of an MPC controller with a kinematic model. However, it is different as the discretization error actually improved their kinematic model, while in this thesis, it likely just made the dynamic trailer model overestimate the trailer states.

Time horizon The largest difference of performance is found for the time horizon. When it is lowered below $\sim$3 s, the trailer error starts to rapidly increase and at 1 s it becomes more than five times larger than the baseline error. At the same time, the tractor error decreases slightly, although much less than the trailer error increases. The cause of this is likely that the shorter time horizon removes the ability of the MPC to deviate from the maneuver in a calculated way, as it is no longer aware of how the path changes ahead. This is probably why the error starts to increase around 3 s, as that equals a prediction distance of $\sim$71 m for 85 km/h, which is also the lookahead distance required to see the second lane change before the first has started. Interestingly, as the MPC uses the Riccati matrix as the terminal weight, its behavior will approximate the LQ controller for lower time horizons. This can be seen as the LQ in the previous sections tends to greedily reduce the tractor error, at the cost of an increased trailer error. However, as the controllers are slightly differently tuned, and because of the feedforward term in the LQ controller, the performance is not exactly the same.

4.2.4 Robustness evaluation

The properties of a semitrailer are highly dependent on several factors. Some of these include static features that vary depending on the manufacturer and model. For example: wheelbase, track width, number of axles, et cetera. Other factors are more related to the cargo, such as the total weight and distribution of load. Additionally, the properties of a trailer are also affected by changes in the environment. Notably, the road coefficient of friction affects the handling stability of the vehicle and varies depending on the current road and weather conditions. These factors play a major role in the overall stability of the vehicle, and there is a wealth of literature regarding the stability properties for various tractor-trailer combinations, [11, 13, 15, 28, 32, 47].

For a freight moving truck, its task is performed with interchangeable trailers. Since the properties of trailers may vary, the controllers should be evaluated under these varying conditions. This is done by changing the values of selected parameters in the simulation environment. The parameters of interest are longitudinal position for trailer center of mass (COM), trailer inertia and road coefficient of friction. The parameters are chosen due to their natural changeability, and presumably, major influence on the vehicle behavior and handling stability.

Using both the LQ and MPC controllers with the dynamic trailer model, the tests are run for the 100 m double lane change at 85 km/h. Furthermore, a conservative tuning of the MPC controller is created to see if performance during large parameter uncertainties can be improved.

Controller performance against uncertainty in position of trailer COM is done by moving it as far back as 3 m from the nominal position and up to 3 m in front of it. Testing for performance during uncertainty in trailer inertia is done by varying the mass of the trailer between 40 % to 140 % of its nominal value (31 610 kg), and scaling the trailer moment of inertias linearly with the mass. Testing for road coefficient of friction uncertainty is done by varying its value from 0.5 to 1.0. The lowest friction corresponds to driving on a wet earth road, and the highest to driving on dry asphalt [29].

LQR performance

The following section presents the LQ controller's performance under parameter uncertainty.

Trailer load distribution In Figure 4.21, the performance of the LQ controller is presented when longitudinal position of the trailer COM is varied. The results show an increase in both cross-track errors when moving the COM rearwards. When moving the COM forwards, the tractor error increases steadily. For the trailer error, it initially becomes smaller until a critical point is reached when the roll angles become very large. As the trailer COM is moved rearwards, the trailer is more prone to lateral tire force saturation of the axles. This leads to trailer sway which becomes increasingly hard for the controller to handle. As the COM is moved forward, rollover stability is decreased [32]. The large roll angles that are produced greatly influences the overall system and the errors increase accordingly. When moving the trailer COM, 2 m forwards from its nominal position, rollover becomes unavoidable.

It is clear that moving the COM of the trailer generally leads to oscillatory behavior, or in worst case, rollover instability. The controller fails to handle these changes, ultimately leading to a decrease in performance.

Trailer inertia In Figure 4.22, the performance of the LQ controller is presented when the trailer inertia is varied. The results show a steady increase in both cross-track errors and maximum trailer roll angle as the mass increases.

As the mass increases the handling stability of the trailer decreases. This is explained with the cornering stiffnesses of the tires not having a linear relation to the vertical load [21, 13]. Since the relation is not linear, the cornering stiffnesses of the

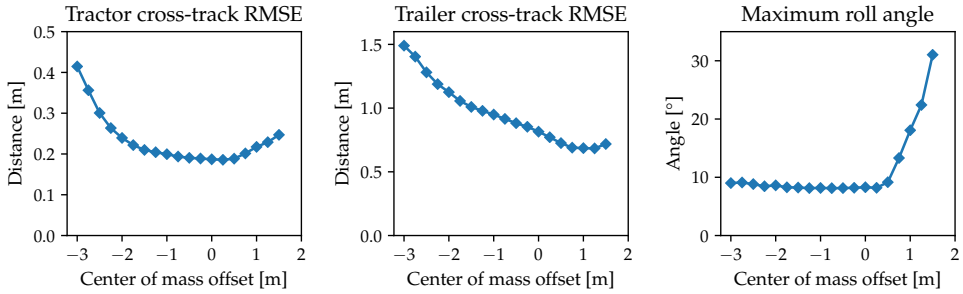

Figure 4.21: The effect of the moving the trailer COM longitudinally on the performance of the LQ controller with a dynamic trailer model.

tires will not increase by the same amount as the mass. Therefore, the damping forces will not increase as much either, making the trailer more prone to sway.

Similarly, to the results that are found in the previous section, the controller does not handle the effects of mass uncertainty well.

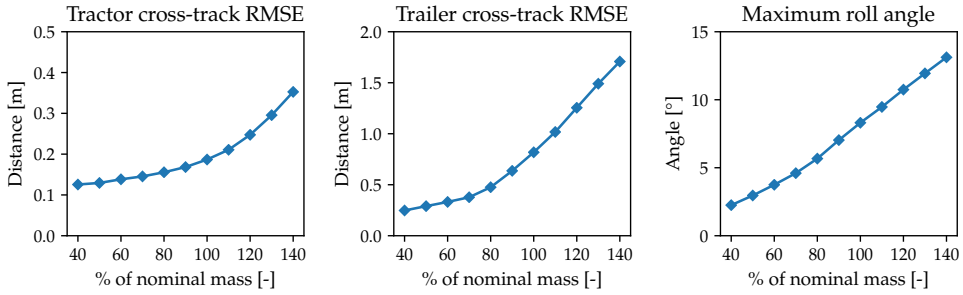

Figure 4.22: The effect of the inertia of the trailer on the performance of the LQ controller with a dynamic trailer model.

Road coefficient of friction In Figure 4.23, the performance of the LQ controller is presented when the road coefficient of friction is varied. As the coefficient of friction is reduced, the vehicle starts to skid, which changes the handling characteristics of the vehicle. The cross-track errors of both the tractor and the trailer increases as the friction decreases, motivated by the loss of traction. The trailer roll angle is almost unaffected by the change in friction. The loss of adhesion means a decrease in the lateral forces on the tires. As these are the main contributers to the rolling dynamics of the trailer, the roll angle maintains mostly unchanged throughout the tests, with a only minimal decrease at the lowest friction values.

From the previous tests it is shown that as trailer sway becomes more prominent, the LQ controller shows a decrease in performance. Similarly to these, the controller fails to react to these changes and underperforms in this case as well.

Summary By varying the parametric values for trailer COM, trailer inertia and road coefficient of friction, the overall vehicle behavior changes. In most cases it leads to decreased handling stability and a trailer that is prone to oscillations. For the LQ controller this becomes problematic, due to its already aggressive behavior (see

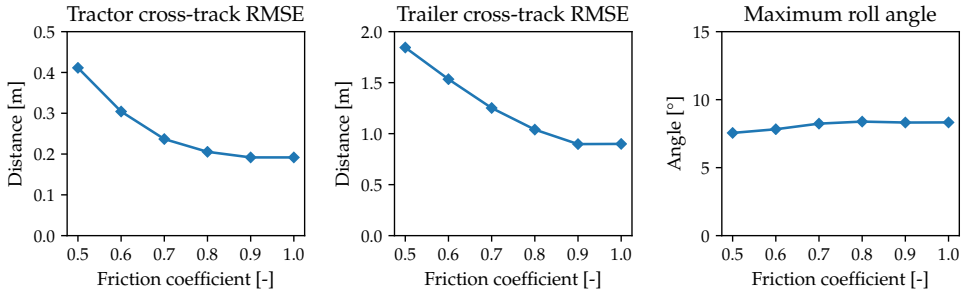

Figure 4.23: The effect of changing the friction coefficient of the road on the performance of the LQ controller with a dynamic trailer model.

Section 4.2.3). As the parametric values are changed, the controller does not adjust its behavior. This is a major drawback for this controller as it shows lack of robustness against uncertainties in these scenarios.

MPC performance

The following section presents the MPC controller's performance under parameter uncertainty. In addition to the standard tuning used in most of the previous experiments, a more conservative tuning is created to see if performance could be improved. All robustness tests therefore include results for both the tuning strategies.

Trailer load distribution In Figure 4.24, the performance of the MPC controller is presented when longitudinal position for the trailer COM is varied. Considering the tractor error, both controllers maintain a near constant value for all tests. The conservative controller has a $\sim$30 % increase in tractor error, which is expected as a more conservative tuning will worsen the path-following abilities. The trailer oscillations that become prominent as the COM is moved increasingly rearwards have a large effect on the trailer errors. The effect is notable for both tuning strategies, though the conservative tuning shows better performance for the tests when the COM is displaced within the range of -2 m to 0 m. As the trailer COM is moved increasingly forwards, large trailer roll angles become prominent for the regularly tuned controller. However, the conservative tuning has a large positive effect on the stability of the system, as it manages to the keep the roll angles low.

With the MPC controller, moving the trailer COM affects the vehicle behavior, but some of these effects may be inhibited by a more conservative tuning. Though this tuning show some performance increase for the trailer error in limited intervals, the positive effects are more prominent in the reduction of the trailer roll angles.

Trailer inertia In Figure 4.25, the performance of the MPC controller is presented when the trailer inertia is varied. Once again, the tractor error maintains near constant values for both controllers, though the conservatively tuned controller shows a slight performance increase when the mass becomes very large. For the trailer errors, the regularly tuned controller performs much better with a small trailer mass than the conservative one. Performance becomes comparable around the trailer's nominal value and upwards.

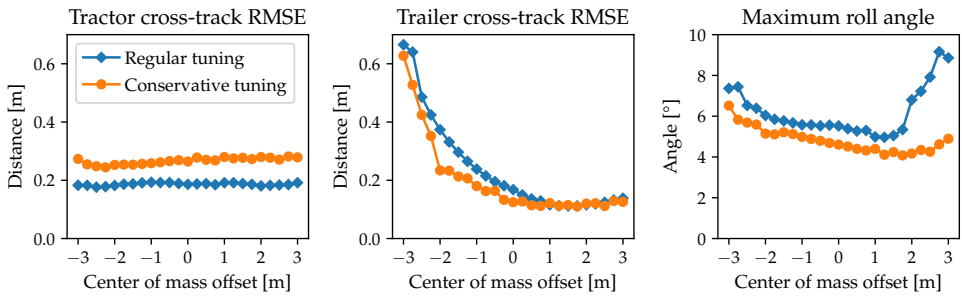

Figure 4.24: The effect of the moving the trailer COM longitudinally on the performance of the regular and conservative MPC controllers with a dynamic trailer model.

The difference between the controllers is more notable for the trailer roll angles. For the regularly tuned controller, the maximum roll angles increases heavily when mass is changed from its nominal value. For larger increases in mass, the roll angles reach critical values. In contrast, the conservative controller maintains much lower roll angles. Although, the roll angles become larger as the mass increase, they never become as large as for the regularly tuned controller.

When varying the trailer inertia, performance of the MPC controller is most negatively affected when its increased beyond its nominal value. The positive effects of the conservatively tuned controller is mostly seen for the trailer roll angles. However, for smaller values of inertia, the conservatively tuned controller has large trailer errors. On the contrary, this is when the regularly tuned controller performs particularly well.

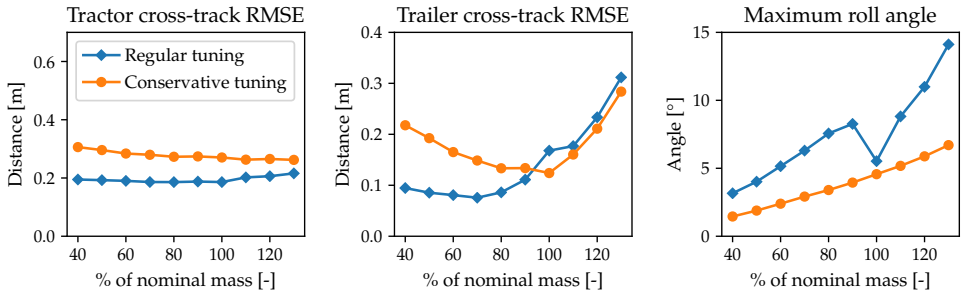

Figure 4.25: The effect of the inertia of the trailer on the performance of the regular and conservative MPC controllers with a dynamic trailer model.

Road coefficient of friction In Figure 4.26, the performance of the MPC controller is presented when the road coefficient of friction is varied. Performance is very consistent for both tractors error and trailer roll angles for both controllers. Most notably, there is a major difference in trailer error when the friction is low. The conservative controller tries much harder to keep the trailer from swinging. At the limits of adhesion, this is extremely beneficial as the risk of skidding is higher. For the lowest friction values, the regularly tuned controller has 0.4 m (200 %) increase in trailer error compared to the conservative one.

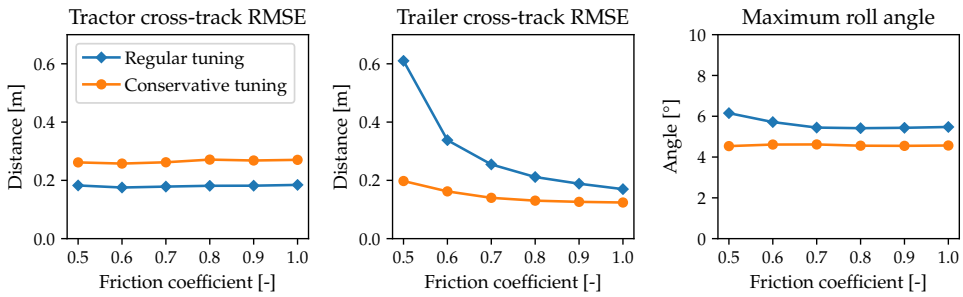

Figure 4.26: The effect of changing the friction coefficient of the road on the performance of the regular and conservative MPC controllers with a dynamic trailer model.

Summary When varying the longitudinal position of trailer COM, trailer inertia and road coefficient of friction, the handling capabilities of the vehicle is largely affected. With the MPC controller, some of these problems become more apparent while others are better handled. Generally, the controller performs well within modest margins of the parameters' nominal values. The largest impact on the controller performance in these tests is when the trailer inertia is increased or when the trailer COM is moved far forward. The boundary values of these parameters are quite extreme, and may not be representable for everyday situations. However, they do well to illustrate more critical trailer configurations. Some of these behaviors, such as large roll angles or excessive yaw motion are inhibited when tuning the MPC controller to act more conservatively. The conservative tuning sacrifices a small tractor error to reduce trailer oscillation. This controller shows a performance increase in some of the edge cases for these tests, especially for a large trailer inertia, a small friction coefficient and a large load displacement in the forward direction. What these tests have in common, is they represent scenarios where the handling stability of the vehicle is low, which the conservative controller handles well. Although the performance increase is mostly noticeable in the extreme cases, it shows that the MPC controller can be modified such that its more robust against uncertainties and possible instabilities.

5 Conclusion

In this thesis, different models of various complexities have been developed for a tractor-trailer vehicle. Additionally, linear quadratic control and model predictive control have been investigated as potential strategies for automatic steering during evasive maneuvers. The main contribution of this work, is the comparative evaluation of dynamic models for lateral control design of tractor-trailer vehicles. In this chapter, the results are summarized, and future works are discussed.

5.1 Conclusions

This thesis has treated modeling and control design of tractor-trailer vehicles. The focus of this work has been the models', and controllers' performance during aggressive maneuvers.

Models of varying complexity of the vehicle have been presented. The models range from a simple kinematic model, to a complex dynamic roll model. It was found that the predictive ability of the models varied extensively. The kinematic models performed exceptionally well for low speeds but struggled as the speed increased. On the contrary, the dynamic models were much better in this regard. Furthermore, the inclusion of a trailer in the model, improved the model's predictive ability. Including roll in the model showed decent results for its ability to predict roll motion, but did not improve prediction of the pose, compared to the model without roll.

Two control methods were used in this thesis, linear quadratic control and model predictive control. With the LQ controller, the best performance was recorded when using dynamic models. The dynamic tractor model performed exceptionally well in keeping the tractor on the path but struggled greatly as trailer sway became more prominent for higher speeds. The best performing model when applying an LQ control strategy was the dynamic trailer model including roll, mainly due to its added capability of making the controller more conservative. Overall, the controller struggled with aggressive behavior, which was mainly explained by its feed-forward term. The aggressive behavior remained a continued issue when evaluating the controller's performance under parameter uncertainty. Although the LQ controller overall has not shown satisfactory performance in this work, the weakness is likely not with the controller, but more so with the path it is required to follow. If the path were generated using the dynamic model (similar to what the MPC does), the performance of the LQ might have been improved, and possibly comparable to the MPC controller.

Similarly, to the LQ controller, the MPC controller enjoyed a performance increase when using the dynamic models. With the MPC controller however, the best performance was gained when using the dynamic trailer model (without roll). In comparison with the LQ controller, the MPC controller performed much better and has shown an overall promising performance for this application. The controller showed decent robustness against parameter uncertainty, which may further be improved with more conservative tuning. The strength of the MPC controller, comes from the fact that it has access to the future reference of the path, making it more robust against sudden changes in the path. This was highly beneficial for the aggressive driving scenarios as the trajectories were on the limits of feasibility.

For both the MPC and LQ controller, the performance improved by directly weighting the approximated trailer deviation. In addition, it made the tuning of the MPC controller much simpler.

5.2 Future work

In this section, future work regarding control of tractor-trailer vehicles is presented.

5.2.1 Modeling improvements

The models presented in Section 2.1, can be extended in several ways to improve their predictive performance. Two large avenues for improvement are the inclusion of nonlinear suspension dynamics to the model with roll, and the inclusion of a nonlinear vertical load dependency on the cornering stiffnesses, as was done in [21]. If nonlinear suspension effects are added, the predictive performance of roll at the brink of rollover could improve. This could make it possible to effectively constrain the lateral load transfer in the MPC controller, and thus reduce the risk of rollover, without making the controller more conservative. Additionally, vertical load dependency on the cornering stiffnesses, can improve the tire model when the weight is shifted to one side of the vehicle.

5.2.2 Robust control

In Section 4.2.4 the robustness of the controllers against parameter uncertainty is analyzed. Additionally, a more conservative MPC controller is used, which shows improved robustness. The usage of robust control techniques, such as *robust MPC*, could be investigated. This can create a conservative controller that handles parameter uncertainty in a more calculated manner.

5.2.3 Combined longitudinal and lateral control

In a realistic evasive maneuver, both steering and braking are important. The interaction between these is significant when the system operates at the limit of traction and stability. Harsh braking can lead to the complete loss of lateral control, but well-executed differential braking can also greatly improve lateral stability. Because of this, it is important to investigate when lateral and longitudinal control cannot be decoupled.

5.2.4 Inclusion of obstacles in MPC

During more aggressive driving, the developed controllers struggle to accurately follow the reference paths. This makes it hard to guarantee that the trajectory of the vehicle is obstacle-free. One way of resolving this issue is the inclusion of obstacles in the MPC controller, which would allow for local re-planning of the trajectory. This is done in [27], but would have to be done using dynamic models to handle aggressive driving.

5.2.5 Planning with dynamic models

Performing re-planning with the MPC controller as described in the previous section is not necessary the most effective method of creating a dynamically feasible trajectory. It will have the typical disadvantage of variational methods, i.e. getting stuck in local minima. Because of this, another possible method is including dynamic models in the typical graph search or incremental search planner. This would allow the use of simpler control techniques, at the cost of a more complex planning cycle.

Bibliography

[1] R Behringer. "The DARPA grand challenge-autonomous ground vehicles in the desert". In: *IFAC Proceedings Volumes* 37.8 (2004), pp. 904–909.

[2] Martin Buehler, Karl Iagnemma, and Sanjiv Singh. *The 2005 DARPA grand challenge: the great robot race*. Vol. 36. Springer, 2007.

[3] Martin Buehler, Karl Iagnemma, and Sanjiv Singh. *The DARPA urban challenge: autonomous vehicles in city traffic*. Vol. 56. springer, 2009.

[4] Brian Paden et al. "A survey of motion planning and control techniques for self-driving urban vehicles". In: *IEEE Transactions on intelligent vehicles* 1.1 (2016), pp. 33–55.

[5] Chang Mook Kang, Seung-Hi Lee, and Chung Choo Chung. "Comparative evaluation of dynamic and kinematic vehicle models". In: *53rd IEEE Conference on Decision and Control*. IEEE. 2014, pp. 648–653.

[6] Moritz Werling, Lutz Groll, and Georg Bretthauer. "Invariant trajectory tracking with a full-size autonomous road vehicle". In: *IEEE Transactions on Robotics* 26.4 (2010), pp. 758–765.

[7] Claudio Altafini. "Some properties of the general n-trailer". In: *International Journal of Control* 74.4 (2001), pp. 409–424.

[8] Claudio Altafini. "Path following with reduced off-tracking for multibody wheeled vehicles". In: *IEEE transactions on control systems technology* 11.4 (2003), pp. 598–605.

[9] Oskar Ljungqvist. *Motion planning and feedback control techniques with applications to long tractor-trailer vehicles*. Vol. 2070. Linköping University Electronic Press, 2020.

[10] Rui Oliveira et al. "Optimization-Based On-Road Path Planning for Articulated Vehicles". Accepted to Proceeding of the IFAC World Congress. Preprint: arXiv:2001.06827. 2020.

[11] Frederick Jindra. "Handling characteristics of tractor-trailer combinations". In: *SAE Transactions* (1966), pp. 378–394.

[12] Sage M Wolfe. "Heavy Truck Modeling and Estimation for Vehicle-to-Vehicle Collision Avoidance Systems". PhD thesis. The Ohio State University, 2014.

[13] MFJ Luijten. "Lateral dynamic behaviour of articulated commercial vehicles". In: *Eindhoven University of Technology* (2010).

[14] Graeme Morrison and David Cebon. "Sideslip estimation for articulated heavy vehicles at the limits of adhesion". In: *Vehicle System Dynamics* 54.11 (2016), pp. 1601–1628.

[15] Roman Kamnik, Friedrich Boettiger, and Ken Hunt. "Roll dynamics and lateral load transfer estimation in articulated heavy freight vehicles". In: *Proceedings of the Institution of Mechanical Engineers, Part D: Journal of Automobile Engineering* 217.11 (2003), pp. 985–997.

[16] Zachary Brock, James Nelson, and Ross L Hatton. "A Comparison of Lateral Dynamic Models for Tractor-Trailer Systems". In: *2019 IEEE Intelligent Vehicles Symposium (IV)*. IEEE. 2019, pp. 2052–2059.

[17] Jarrod M Snider et al. "Automatic steering methods for autonomous automobile path tracking". In: *Robotics Institute, Pittsburgh, PA, Tech. Rep. CMU-RITR-09-08* (2009).

[18] Jason Kong et al. "Kinematic and dynamic vehicle models for autonomous driving control design". In: *2015 IEEE Intelligent Vehicles Symposium (IV)*. IEEE. 2015, pp. 1094–1099.

[19] Fitri Yakub and Yasuchika Mori. "Comparative study of autonomous path-following vehicle control via model predictive control and linear quadratic control". In: *Proceedings of the Institution of Mechanical Engineers, Part D: Journal of automobile engineering* 229.12 (2015), pp. 1695–1714.

[20] Oskar Ljungqvist et al. "Estimation-aware model predictive path-following control for a general 2-trailer with a car-like tractor". In: *arXiv preprint arXiv:2002.10291* (2020).

[21] David John Matthew Sampson. "Active roll control of articulated heavy vehicles". PhD thesis. 2000.

[22] Arnaud JP Miege and David Cebon. "Optimal roll control of an articulated vehicle: theory and model validation". In: *Vehicle system dynamics* 43.12 (2005), pp. 867–884.

[23] Chieh Chen and Masayoshi Tomizuka. "Lateral control of commercial heavy vehicles". In: *Vehicle System Dynamics* 33.6 (2000), pp. 391–420.

[24] BA Jujnovich and D Cebon. "Path-following steering control for articulated vehicles". In: *Journal of Dynamic Systems, Measurement, and Control* 135.3 (2013).

[25] Graeme Morrison and David Cebon. "Combined emergency braking and turning of articulated heavy vehicles". In: *Vehicle system dynamics* 55.5 (2017), pp. 725–749.

[26] Jessica Van Brummelen et al. "Autonomous vehicle perception: The technology of today and tomorrow". In: *Transportation research part C: emerging technologies* 89 (2018), pp. 384–406.

[27] Pedro F Lima. "Optimization-based motion planning and model predictive control for autonomous driving: With experimental evaluation on a heavy-duty construction truck". PhD thesis. KTH Royal Institute of Technology, 2018.

[28] Yunbo Hou. "Roll and Yaw Stability Evaluation of Class 8 Trucks with Single and Dual Trailers in Low-and High-speed Driving Conditions". PhD thesis. Virginia Tech, 2017.

[29] Jo Yung Wong. *Theory of ground vehicles*. John Wiley & Sons, 2008.

[30] Jonathan Y. Goh, Tushar Goel, and J. Christian Gerdes. "Toward Automated Vehicle Control Beyond the Stability Limits: Drifting Along a General Path". In: *Journal of Dynamic Systems, Measurement, and Control* 142.2 (2019).

[31] Stephen M Erlien, Joseph Funke, and J Christian Gerdes. "Incorporating nonlinear tire dynamics into a convex approach to shared steering control". In: *2014 American Control Conference*. IEEE. 2014, pp. 3468–3473.

[32] Christopher B Winkler. *Rollover of heavy commercial vehicles*. Tech. rep. Society of Automotive Engineers, Warrendale, Pa., 1999.

[33] Caizhen Cheng and David Cebon. "Parameter and state estimation for articulated heavy vehicles". In: *Vehicle System Dynamics* 49.1-2 (2011), pp. 399–418.

[34] Hans Pacejka. *Tire and vehicle dynamics*. Elsevier, 2005.

[35] Chieh Chen and Masayoshi Tomizuka. "Dynamic modeling of tractor-semitrailer vehicles in automated highway systems". In: (1995).

[36] Daniel Wesemeier and Rolf Isermann. "Identification of vehicle parameters using stationary driving maneuvers". In: *Control Engineering Practice* 17.12 (2009), pp. 1426–1431.

[37] Mario Zanon, Janick V Frasch, and Moritz Diehl. "Nonlinear moving horizon estimation for combined state and friction coefficient estimation in autonomous driving". In: *2013 European Control Conference (ECC)*. IEEE. 2013, pp. 4130–4135.

[38] Janick V Frasch et al. "Moving horizon observation for autonomous operation of agricultural vehicles". In: *2013 European Control Conference (ECC)*. IEEE. 2013, pp. 4148–4153.

[39] Alessandro De Luca, Giuseppe Oriolo, and Claude Samson. "Feedback control of a nonholonomic car-like robot". In: *Robot motion planning and control*. Springer, 1998, pp. 171–253.

[40] Roger Skjetne and Thor I Fossen. "Nonlinear maneuvering and control of ships". In: *MTS/IEEE Oceans 2001. An Ocean Odyssey. Conference Proceedings (IEEE Cat. No. 01CH37295)*. Vol. 3. IEEE. 2001, pp. 1808–1815.

[41] Torkel Glad and Lennart Ljung. *Reglerteori: flervariabla och olinjära metoder*. Studentlitteratur, 2003.

[42] Moritz Diehl et al. "Fast direct multiple shooting algorithms for optimal robot control". In: *Fast motions in biomechanics and robotics*. Springer, 2006, pp. 65–93.

[43] Andreas Wächter and Lorenz T Biegler. "On the implementation of an interior-point filter line-search algorithm for large-scale nonlinear programming". In: *Mathematical programming* 106.1 (2006), pp. 25–57.

[44] Gionata Cimini and Alberto Bemporad. "Exact complexity certification of active-set methods for quadratic programming". In: *IEEE Transactions on Automatic Control* 62.12 (2017), pp. 6094–6109.

[45] Daniel Arnström and Daniel Axehill. "A Unifying Complexity Certification Framework for Active-Set Methods for Convex Quadratic Programming". Preprint: arXiv:2003.07605. 2020.

[46] Joel A E Andersson et al. “CasADi – A software framework for nonlinear optimization and optimal control”. In: *Mathematical Programming Computation* (In Press, 2018).

[47] Gonzalo Moreno et al. “Stability of Heavy Articulated Vehicles: Effect of Load Distribution”. In: *Transportation research procedia* 33 (2018), pp. 211–218.